

Energy Materials Telecommunications

# **Biosignals Detection Using MIMO Radar System**

## **Détection de biosignaux à l'aide du système radar**

### **MIMO**

By

Halima Abd Alla EL Grari

Dissertation or thesis presented for obtaining the degree of Master of Science (M.Sc.) in  
Telecommunications

#### **Evaluation Jury**

Président du jury et  
examineur interne

Shervin, Vakili  
Énergie Matériaux Télécommunications  
INRS

Examineur externe

MOURAD, NEDIL  
Université du Québec en Abitibi-  
Témiscamingue

Directeur de recherche

Tarek, Djerafi  
Énergie Matériaux Télécommunications  
INRS

## **ACKNOLDEGMENT**

---

First and foremost, I would like to extend my deepest gratitude to my principal professor Tarek Djerafi, his patience and enlightening instruction allowed me to see who a real professor is. This thesis would not have been possible without him. I also extend my thanks to his professionalism and work attitude that impressed me deeply. Finally, I would like to thank all my friends, especially Ahlam Said and Adel Taghdi. Thank you for your support and guidance.

## DEDICATION

---

### **To my wonderful family**

I dedicate the success of my thesis to my mother and to the memory of my father whose encouragement made this academic journey possible for my future contribution in my field of telecommunication and biomedical applications.

## RÉSUMÉ

---

L'émergence de la technologie radar dans le domaine médical promet d'optimiser les soins de santé grâce à une meilleure expérience patient, de réduire les coûts, de gagner du temps et d'augmenter la précision. Par rapport aux approches traditionnelles, la nature non invasive et sans contact de la technologie radar apporte un changement transformateur à la façon dont les signes vitaux des patients sont surveillés. Cependant, la technologie de détection vitale basée sur le radar est confrontée à des défis, notamment le fait que l'état de l'art ne couvre que le cœur et la respiration. Cette thèse vise à relever ces défis en mesurant les ondes électromagnétiques et l'interaction dialectique des tissus humains ; déterminer la fréquence de transport optimale et mesurer directement l'activité cardiaque et électrique à l'aide d'un système radar MIMO multi-entrées multi-sorties. Nous avons conçu et développé un système de capteur radar sans contact combiné à divers algorithmes pour mesurer de manière exhaustive les conditions respiratoires et cardiovasculaires. Les résultats expérimentaux montrent que nos mesures de signaux biomédicaux sans contact atteignent une grande précision dans la détection des signes vitaux et des événements électriques cardiaques et cérébraux. Ces résultats indiquent qu'un seul système a le potentiel de détecter des biosignaux en particulier l'ECG, l'EEG, la RR et la FC simultanément sans contact et continue et précise. L'évaluation des performances du système radar MIMO proposé est validée expérimentalement et comparée à des valeurs standards obtenues par des dispositifs standards. Enfin, nous avons démontré la capacité du système à mesurer directement les signaux bioélectriques.



## ABSTRACT

---

The emergence of radar technology in the medical field promises to optimize healthcare through better patient experience, reduce costs, save time and increase accuracy. Compared to traditional approaches, the non-invasive, non-contact nature of radar technology is bringing a transformative change to the way patient vital signs are monitored. However, radar-based vital detection technology faces challenges, including the fact that the state of the art only covers the heart and respiration. This thesis aims to address these challenges by measuring electromagnetic waves and the dialectical interaction of human tissues; determine the optimal transport frequency and directly measure cardiac and electrical activity using a multi-input multi-output MIMO radar system. We have designed and developed a non-contact radar sensor system combined with various algorithms to comprehensively measure respiratory and cardiovascular conditions. Experimental results show that our non-contact biomedical signal measurements achieve high accuracy in detecting vital signs and cardiac and brain electrical events. These results indicate that a single system has the potential to detect biosignals in particular ECG, EEG, RR and HR simultaneously non-contact and continuous and accurate. The performance evaluation of the proposed MIMO radar system is experimentally validated and compared to standard values obtained by standard devices. Finally, we demonstrated the ability of the system to directly measure bioelectrical signals.



## 0 Synopsis

---

### Détection de biosignaux à l'aide du système radar MIMO

#### 0.1 Introduction

Ce chapitre présente une brève introduction à la technologie des capteurs radar Doppler sans contact et non-invasifs. Il met en évidence ses avantages et ses applications répandues dans le domaine médical. Les intérêts et les raisons qui nous ont amenés à entreprendre cette recherche sont ensuite exprimés. Par la suite, les objectifs et les défis de la recherche sont décrits de manière concise. Les principales contributions à la thèse sont répertoriées. Enfin, l'organisation et la structure de la thèse sont présentées. La détection radar Doppler, une méthode non-invasive conçue pour détecter les signes vitaux des patients dans les centres de soins, les maisons et les zones sinistrées, peut améliorer le diagnostic et éclairer les traitements ciblés, un saut vers la médecine de précision. Ce travail, qui aspire à concevoir et à développer un système de détection radar médical, vise à accroître l'utilisation de la détection et de la mesure sans contact des signaux biologiques. Cependant, la mise en œuvre généralisée du radar médical est confrontée à des défis tels que : l'ambiguïté due au manque de portée, les limitations de l'imagerie en raison du court temps d'observation et la faible résistance aux interférences - le rapport signal/bruit prédominant au SNR. Les inconvénients susmentionnés peuvent être contournés en réalisant des simulations spécifiques et des expériences en laboratoire.

Différentes approches, notamment HFSS, MatLab, ADS, des modèles de réseaux de neurones et divers algorithmes, sont utilisées pour détecter les biosignaux, principalement la respiration et le rythme cardiaque. Grâce à l'évaluation et à l'intégration desdites approches, des informations cardiaques et respiratoires à partir de signaux en bande de base peuvent alors être obtenues avec une grande précision. La mesure quantitative de l'interaction entre l'EM et les tissus humains est un facteur contribuant à l'amélioration des capacités et à la réduction des coûts dans le développement de nouvelles technologies de fabrication d'antennes et de radars. L'utilisation du radar dans les applications médicales comme méthode de surveillance des inter fonctions et des mouvements d'organes a commencé lorsque N. S. NAMEROW a déposé un brevet en 1969 aux États-Unis [47]. Cette technologie a depuis évolué pour détecter les mouvements physiologiques et les paramètres de santé. Plus tard, C.G. Brown Etal a déposé un brevet en 1971 pour mesurer le rayonnement du champ électrique des corps

vivants [105]. Le radar Doppler, choisi comme modèle pour développer ces systèmes de surveillance, permet des mesures sans contact avec la peau en donnant une alerte plus rapide en cas de dysfonctionnement physiologique et organique humain, c'est-à-dire les signes vitaux. La physiologie basée sur le radar et la mesure du biosignal dépendent en partie de la capacité du système radar à extraire des informations précieuses sur une structure complexe telle que le corps humain. De plus, le capteur radar s'appuie sur l'effet de modulation du signal électromagnétique radar émis lorsqu'il entre en contact avec le corps humain. La compréhension des fonctions et propriétés physiologiques du corps humain (propriétés dépendant de la fréquence) ainsi que la compréhension et la quantification de l'interaction entre le corps humain et les ondes électromagnétiques font partie intégrante de ce travail. Cela conduit à déterminer la fréquence porteuse optimale.

## **0.2 Motivation**

Cette thèse fait partie d'un vaste projet dont l'objectif est de détecter bio mécaniquement et de mesurer directement les signaux électriques de sujets humains vivants pour faciliter le diagnostic médical, le traitement et le suivi. Ces patients devaient souvent traverser des terrains difficiles pour atteindre ces centres de santé. Les signes vitaux sont encore mesurés manuellement ce qui ajoute de la charge au personnel et augmente les risques dans les périodes de pandémie. Cela conduit souvent à un temps d'attente prolongé pour le patient. De plus, une nouvelle étude menée par des chercheurs canadiens a démontré que les longs délais d'attente affectent non seulement la satisfaction des patients, mais augmentent également le risque de décès et de réadmission à l'hôpital pour les patients qui ont obtenu leur congé du service des urgences. À notre avis, la plupart des procédures médicales de suivi pourraient et facilement être effectuées à distance à l'aide de radars médicaux et d'outils de base de l'« Internet des objets » (IoT) à un faible coût et avec un taux d'efficacité plus élevé.

## **0.3 Objectifs et défis de la recherche**

Les objectifs les enjeux de ce projet sont de :

- L'optimisation de divers éléments radar médicaux pour concevoir et développer un système de détection sans contact qui met l'accent sur la haute précision et la meilleure expérience des patients.
- L'étude des effets de la fréquence, de la puissance, du type d'antenne, de la polarisation, du type de corps, de la position du corps, de la distance entre l'antenne

et le sujet, des techniques de traitement du signal et de la position de l'antenne sur la précision de la surveillance des signes vitaux.

- L'exploitation de l'interaction des ondes électromagnétiques et des tissus humains. pour détecter et mesurer directement les activités électriques du cœur et du cerveau.
- Tenir compte du bruit ambiant et des mouvements brusques du patient et de leur effet sur l'acquisition et le traitement du signal
- Examiner et développer de nouvelles techniques pour atteindre une fréquence optimale.

Les défis les plus importants dans la réalisation du projet étaient : l'ambiguïté, les limitations du au court temps d'observation et la faible résistance aux interférences avec un rapport signal/bruit prédominant au SNR.

#### **0.4 Contribution à la thèse**

Les principales contributions de cette thèse sont listées comme suit :

- L'étude des écarts importants entre les valeurs utilisées dans les travaux antérieurs et celles répertoriées dans les références des autorités médicales réputées telles que l'American Heart Association.
- Étude approfondie de l'interaction des EM et des tissus humains. Et intégrer les résultats et les observations tout en sélectionnant la fréquence optimale pour détecter les rythmes respiratoire et cardiaque.
- À notre connaissance, il s'agit du premier travail effectué sur la mesure directe des activités électriques à l'aide de systèmes radar à entrées multiples et sorties multiples.

Les autres contributions incluent :

- Réalisation d'expériences sur un large éventail de sujets d'âge, de sexe, de problèmes de santé différents et plus particulièrement d'états cardiaques et cérébraux. Cela a conduit à renforcer l'intégrité de nos méthodes et de nos résultats en général.
- Guidés par les résultats obtenus à partir de la mesure des ondes EM et de l'interaction des tissus humains, des expériences de laboratoire, des logiciels de simulation et des algorithmes ont été utilisés pour mesurer la fréquence respiratoire RR et la fréquence cardiaque HR. De plus, dans cette thèse, nous avons utilisé le rythme cardiaque standard de la fréquence respiratoire répertorié dans les références des autorités médicales réputées telles que l'American Heart Association pour éviter les écarts et les limitations importants présents dans les travaux précédents.

Même si la détection de la fréquence cardiaque présente un défi principal habituel pour la détection des signes vitaux, car la respiration induit un mouvement de la paroi thoracique comparativement plus important que le rythme cardiaque, une extraction transparente du signal respiratoire tout en mesurant avec précision la fréquence cardiaque. Les valeurs de mesure expérimentales obtenues étaient : la fréquence cardiaque est de 72 bpm, et la respiration est de 16 bpm. Pour illustrer davantage l'effet des interférences respiratoires sur la détection de la fréquence cardiaque, nous avons effectué une deuxième expérience par l'arrière. L'amplitude du signal de battement cardiaque détecté depuis l'arrière était beaucoup plus élevée que lorsqu'il était mesuré depuis l'avant. Cela indique clairement moins d'interférences des fondamentaux de la respiration et de ses harmoniques sur les signaux de battement de coeur.

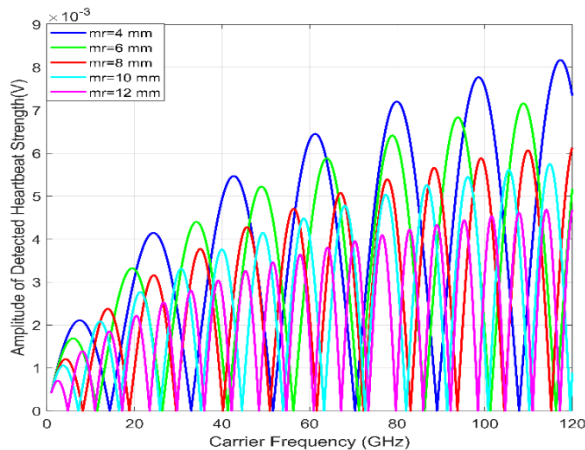


**Figure 0.1. Illustration Amplitude du signal de battement cardiaque détecté depuis la face avant.**

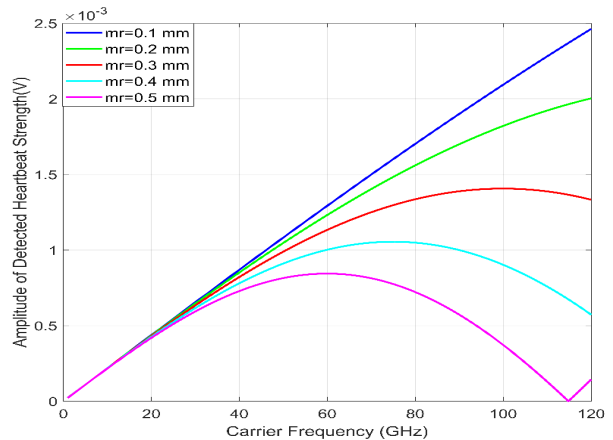


**Figure 0.2 Amplitude du signal de battement cardiaque détecté à l'arrière.**

Nous avons en outre exploré la possibilité de détecter directement l'activité cardiaque et cérébrale bioélectrique. Le système radar MIMO multi-entrées multi-sorties exploite les deux émetteurs et les deux récepteurs intégrés aux antennes électriques. Le logiciel ADS a été utilisé pour simuler le processus de mesure MIMO. Étant donné que les champs magnétiques dans la gamme des basses fréquences considérées étaient extrêmement faibles - allant de 0 à 3 kHz, leur détection nécessite un équipement de laboratoire assez étendu. Les premiers résultats de mesure (figure 0.3 pour le ECG et figure 0.4 pour le EEG) obtenus s'avèrent toutefois prometteurs pour la poursuite du développement du système de détection directe.

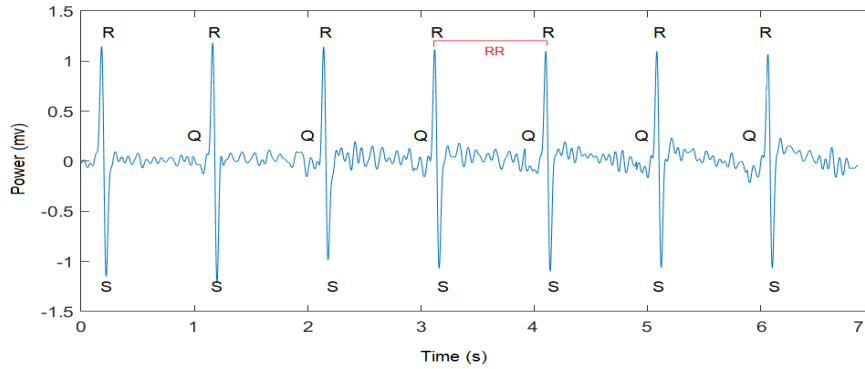


Figure 0.3 Signal ECG obtenu à partir du système radar MIMO. Il montre la représentation graphique de l'activité électrique du cœur. Cela a conduit à d'autres extractions de fonctionnalités. L'intervalle RR commence au pic d'une onde R et se termine au pic de l'onde R suivante. Il représente le temps entre deux complexes QRS. La hauteur de la déviation représente également la quantité d'activité électrique circulant. Plus la déviation est élevée, plus la quantité d'activité électrique est importante. L'onde R est nettement supérieure à l'onde S. Cela suggère une dépolarisation. Le complexe QRS représente la dépolarisation des ventricules. Il rééchantillonne étroitement celui d'un ECG normal. Il apparaît, comme le montre le graphique, sous la forme de trois ondes étroitement liées, à savoir les ondes Q, R et S.

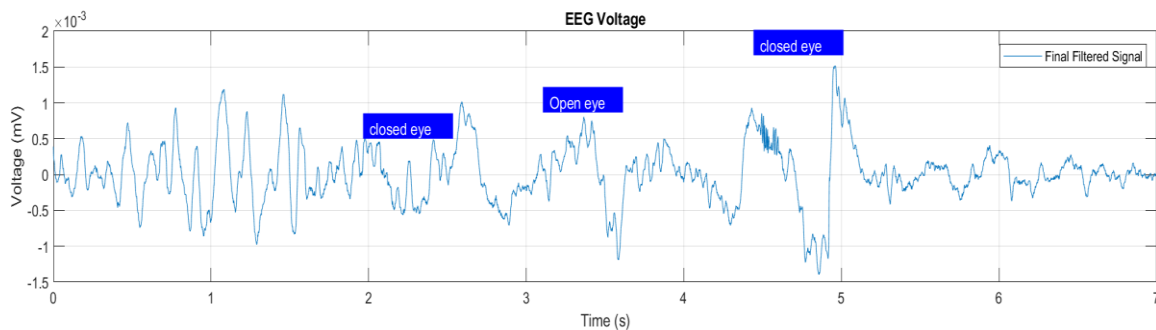


Figure 0.4 Un tracé des résultats du signal EEG obtenu à partir du système radar MIMO sur un graphique temps (en secondes) en fonction de la tension (en mV). Cela montre que le signal avec les cellules cérébrales se comporte beaucoup à la manière d'une propagation d'onde conventionnelle. Le signal EEG est une manifestation de l'activité cérébrale d'un sujet humain en bonne santé - croisement avec l'onde bêta illustrée à la figure 6.4 (esprit occupé et actif). À gauche du graphique, les yeux du sujet étaient fermés et à droite du graphique, les yeux du sujet étaient grands ouverts. La fluctuation constante à faible, c'est-à-dire lorsque les yeux étaient fermés et la fluctuation élevée lorsque les yeux étaient grands ouverts. Le degré de fluctuation indique le niveau d'activité cérébrale ou l'état d'esprit.

## 0.5 Organisation des thèses

Cette thèse est structurée comme suit:

Le chapitre 1 donne un aperçu général du développement du radar et de sa mise en œuvre médicale dans la détection de signaux biologiques. Il met en évidence la portée et le cadre de la

thèse, y compris la définition du contexte de l'étude, la motivation, la contribution, les objectifs, les défis et l'organisation de la thèse.

Le chapitre 2 introduit les principes et les discussions sur l'utilisation du radar doppler pour la détection des signaux physiologiques et vitaux. Il décrit les fonctions les propriétés biologiques du corps humain, en particulier les activités cardiovasculaires, c'est-à-dire mécaniques et électriques. Il présente les deux catégories d'appareils de détection des signes vitaux, c'est-à-dire les techniques basées sur le contact et sans contact.

Le chapitre 3 présente une étude approfondie et des approches de mesure des ondes électromagnétiques et de l'interaction des tissus humains. Il présente l'architecture et le fonctionnement du radar Doppler et fournit une liste et une discussion sur l'état de l'art pertinent, y compris la limitation des approches précédentes de mesure des signaux vitaux.

Le chapitre 4 illustre en détail les travaux entrepris pour déterminer la fréquence porteuse optimale tout en mesurant la respiration et la fréquence cardiaque. Ce chapitre présente également l'utilisation du système de conception avancée (ADS) pour effectuer la mesure et le traitement des biosignaux détectés en bande de base, c'est-à-dire la fréquence respiratoire, le rythme cardiaque et l'ECG. Des expériences de laboratoire à l'INRS et leurs résultats sont également présentés dans ce chapitre.

Le chapitre 5 effectue une détection directe du signal cardio-électrique via un radar MIMO. Et il aborde brièvement la corrélation des signaux électromécaniques cardiaques. Des diagrammes et des graphiques pour illustrer les événements cycliques cardiaques sont également présentés.

Le chapitre 6 présente l'électroencéphalogramme comme un outil crucial dans la surveillance et le diagnostic du cerveau. Une détection directe du signal électrique cérébral est effectuée à l'aide du système radar MIMO.

Le chapitre 7 fournit les conclusions, les recommandations et les travaux futurs possibles.

# CONTENTS

---

<b>ACKNOWLEDGMENT</b> .....	<b>III</b>
<b>DEDICATION</b> .....	<b>IV</b>
<b>RÉSUMÉ</b> .....	<b>V</b>
<b>ABSTRACT</b> .....	<b>VII</b>
<b>0 SYNOPSIS</b> .....	<b>IX</b>
0.1 INTRODUCTION .....	IX
0.2 MOTIVATION .....	X
0.3 OBJECTIFS ET DÉFIS DE LA RECHERCHE .....	X
0.4 CONTRIBUTION À LA THÈSE .....	XI
0.5 ORGANISATION DES THÈSES .....	XIII
<b>CONTENTS</b> .....	<b>XV</b>
<b>LISTE OF FIGURES</b> .....	<b>XVII</b>
<b>LIST OF TABLE</b> .....	<b>XIX</b>
<b>LISTE DES ABRÉVIATIONS</b> .....	<b>21</b>
<b>1 GENERAL AND DEFINITION OF THE CONTEXT OF RESEARCH</b> .....	<b>22</b>
1.1 INTRODUCTION .....	22
1.2 MOTIVATION .....	23
1.3 RESEARCH OBJECTIVES AND CHALLENGES .....	23
1.4 THESIS CONTRIBUTION .....	24
1.5 THESIS ORGANISATION .....	24
<b>2 PRINCIPLES AND IMPLEMENTATION OF DOPPLER RADAR</b> .....	<b>26</b>
2.1 DOPPLER RADAR BASED HEALTHCARE SYSTEM .....	26
2.2 PHYSIOLOGY AND VITAL SIGNAL MEASUREMENT USING RADAR .....	26
2.2.1 <i>Radar Sensor Systems</i> .....	27
2.2.2 <i>Principles and Components of the CW Doppler Radar System</i> .....	28
2.2.3 <i>Human Body Physiological Functions and Properties</i> .....	29
2.3 VITAL SIGNAL .....	30
2.3.1 <i>Respiration Rate</i> .....	31
2.4 HEART RATE .....	31
2.4.1 <i>Cardiovascular Activity</i> .....	32
2.4.2 <i>Electrical Impulses of the Heart</i> .....	34
2.4.3 <i>Electrocardiogram ECG</i> .....	34
2.4.4 <i>Electroencephalography EEG</i> .....	35
2.5 DEVICES AND TECHNIQUES USED IN MEASURING BIOSIGNAL .....	35
2.5.1 <i>Implantable Sensor (Invasive Techniques)</i> .....	35
2.5.2 <i>Non-invasive Techniques</i> .....	36
<b>3 STUDY OF ELECTROMAGNETIC WAVES AND HUMAN TISSUES INTERACTION</b> .....	<b>38</b>

3.1	INTERACTION OF ELECTROMAGNETIC RADIATION WITH THE HUMAN BODY .....	38
3.2	SIMULATION AND MEASUREMENT OF BODY TISSUES AND EM INTERACTION.....	39
3.3	DOPPLER RADAR AND THE OPTIMIZATION OF HEALTHCARE .....	44
3.4	NOISE AND RADAR SENSING .....	45
3.5	ARCHITECTURE AND OPERATION OF CW DOPPLER RADAR.....	46
3.6	RELEVANT STATE OF THE ART .....	47
3.7	LIMITATION OF PVIOUS VITAL SIGNAL MEASUREMENT APPROACHES.....	50
<b>4</b>	<b>DETERMINING THE OPTIMAL CARRIER FREQUENCY TO DETECT RR AND HR.....</b>	<b>51</b>
4.1	OPTIMAL FREQUENCY MEASURMENT.....	51
4.2	DETECTION OF HEARTBEAT AND RESPIRATION USING ADS .....	53
4.3	LAB EXPERIMENT AND RESULTS.....	55
4.3.1	<i>Experimental Procedure</i> .....	56
<b>5</b>	<b>DIRECT DETECTION OF BIOELECTRICAL SIGNAL VIA MIMO RADAR .....</b>	<b>61</b>
5.1	BIOLOGICAL SIGNAL IN THE HUMAN BODY.....	61
5.2	CARDIO ELECTRO-MECHANICAL EVENTS .....	61
5.2.1	<i>Cardiac Mechanical Signal</i> .....	63
5.2.2	<i>Cardiac Electrical Signal</i> .....	64
5.3	CARDIO ELECTRICAL AND MECHANICAL SIGNALS CORRELATION .....	66
5.4	DIRECT MEASURMENT OF CARDIAC ELECTRICAL SIGNAL ECG .....	67
<b>6</b>	<b>ELECTROENCEPHALOGRAPH SIGNAL DETECTION USING MIMO RADAR SYSTEM.....</b>	<b>70</b>
6.1	BRAIN ACTIVITIES .....	70
6.2	ELECTROENCEPHALOGRAPHY .....	71
6.3	EEG MONITORING USING CONTACTLESS MIMO RADAR SYSTEM .....	72
<b>7</b>	<b>CONCLUSION .....</b>	<b>74</b>
7.1	RECOMANDATION AND FUTURE WORK .....	75
<b>8</b>	<b>REFRENCES .....</b>	<b>77</b>
	<b>PUBLICATIONS .....</b>	<b>85</b>

## LISTE OF FIGURES

---

FIGURE 0.1	ILLUSTRATION AMPLITUDE DU SIGNAL DE BATTEMENT CARDIAQUE DÉTECTÉ DEPUIS LA FACE AVANT. ....	XII
FIGURE 0.2	AMPLITUDE DU SIGNAL DE BATTEMENT CARDIAQUE DÉTECTÉ À L'ARRIÈRE. ....	XII
FIGURE 0.3	SIGNAL ECG OBTENU À PARTIR DU SYSTÈME RADAR MIMO. ....	XIII
FIGURE 0.4	UN TRACÉ DES RÉSULTATS DU SIGNAL EEG OBTENU À PARTIR DU SYSTÈME RADAR MIMO .....	XIII
FIGURE 2.1	GLOBAL CAUSES OF DEATH 2000, 2010, 2019. ....	26
FIGURE 2.2	DOPPLER RADAR OPERATION MODES .....	29
FIGURE 2.3	ANTERIOR VIEW OF THE FRONTAL SECTION OF THE HEART .....	32
FIGURE 2.4	THE CARDIAC CYCLE EVENTS FOR THE LEFT PUMP OF THE HEART FOR TWO COMPLETE CYCLES.....	34
FIGURE 2.5	THE TRADITIONAL ECG MEASUREMENT .....	37
FIGURE 2.6	EEG DEVICE MEASUREMENTS .....	37
FIGURE 3.1	SHOWN PROPAGATION OF ELECTROMAGNETIC WAVE .....	38
FIGURE 3.2	MEASUREMENTS OF THE CONDUCTIVITY (S/M) OF VARIOUS BODY TISSUES BY GABRIEL AND GESTBLOM .....	39
FIGURE 3.3	GRAPH OF THE PERMITTIVITY ( $\epsilon$ ) OF VARIOUS BODY TISSUES AT DIFFERENT FREQUENCIES.....	41
FIGURE 3.4	GRAPH OF THE DIELECTRIC LOSS TANGENT OF VARIOUS BODY TISSUES AT DIFFERENT FREQUENCIES.....	41
FIGURE 3.5	(A) MULTILAYERED FLAT TISSUE MODEL AND (B) MODEL PREDICTED ATTENUATION OF PULSE-ECHO INTENSITY	42
FIGURE 3.6	ILLUSTRATED TWO SIDES OF THE BOX ARE PAIRED WITH MASTER AND SLAVE BOUNDARY CONDITIONS AND THE TOP SIDE IS CONSIDERED AS OPEN .....	43
FIGURE 3.7	MAGNITUDES OF PENETRATION AND REFLECTION OF ELECTROMAGNETIC WAVES THROUGH THE HUMAN BODY.	44
FIGURE 3.8	A SIMPLIFIED BLOCK DIAGRAM OF DOPPLER-RADAR BASED VITAL SIGNS MONITORING. ....	47
FIGURE 3.9	AMPLITUDE OF DETECTED HEARTBEAT SIGNAL VS CARRIER FREQUENCY .....	51
FIGURE 4.1	AMPLITUDE OF DETECTED HEARTBEAT SIGNAL FROM THE FRONT SIDE. ....	53
FIGURE 4.2	AMPLITUDE OF DETECTED HEARTBEAT SIGNAL THE BACK SIDE .....	53
FIGURE 4.3	COMPARISON BETWEEN THE BESSEL FUNCTION OF THE FIRST KIND OF ORDER 1 AND THE LINEAR APPROXIMATION FOR THE MOVEMENT AMPLITUDE CASES OF (A) HEARTBEAT; (B) RESPIRATION.....	54
FIGURE 4.4	AN ADS SCHEMATIC DIAGRAM OF DOPPLER RADAR SYSTEMS TO SIMULATE THE DETECTION OF BIOSIGNALS .	55
FIGURE 4.5	SIMULATED MEASUREMENTS OF RESPIRATION RATE RR, AND HEART RATE HR PERFORMED USING ADS .....	56

FIGURE 4.6,A	A BLOCK DIAGRAM ILLUSTRATES THE MULTI-INPUT MULTI OUTPUT SETUP OF MIMO RADAR SYSTEM EMPLOYED TO DETECT BIOSIGNALS .....	57
FIGURE 4.6,B	SHOWS THE BASIC STEPS OF THE PREPROCESSING.....	57
FIGURE 4.7	SHOWS THE BASIC STEPS OF THE PREPROCESSING INCLUDING.....	58
FIGURE 4.8	TIME DOMAIN WAVEFORM OF THE RADAR RESULT. ....	59
FIGURE 4.9	FFT SIGNAL OF TIME DOMAIN OUTPUT.....	59
FIGURE 4.10	RESPIRATORY SIGNAL.....	59
FIGURE 4.11	FFT OF RESPIRATION SIGNAL.....	59
FIGURE 4.12	HEART RATE SIGNAL.....	59
FIGURE 4.13	FFT OF HEARTBEAT SIGNAL. ....	59
FIGURE 5.1	EVENTS OF THE CARDIAC CYCLE.....	63
FIGURE 5.2	SHAPE OF ACTION POTENTIALS FOR HEART. ....	64
FIGURE 5.3	ELECTROPHYSIOLOGY OF THE CARDIAC MUSCLE CEL.....	65
FIGURE 5.4	RELATIONSHIP BETWEEN THE ELECTRICAL AND MECHANICAL CHARACTERISTICS OF THE HEART ACTIVITY.....	67
FIGURE 5.5	A BLOCK DIAGRAM SHOWING THE INTERCONNECTION OF THE COMPONENTS OF THE PROPOSED SYSTEM.....	68
FIGURE 5.6	SCHEMATIC DIAGRAM OF MIMO RADAR SYSTEM ILLUSTRATES THE DIRECT MEASUREMENT OF HEART ELECTRICAL ACTIVITY VIA ADS.....	69
FIGURE 5.7	ECG SIGNAL OBTAINED FROM MIMO RADAR SYSTEM.. ....	69
FIGURE 6.1	BIOLOGICAL STRUCTURE OF A TYPICAL NEURON. ....	70
FIGURE 6.2	UNDERSTANDING NEURONAL ACTIVITY. ....	71
FIGURE 6.3	ILLUSTRATION OF DIFFERENT TYPES OF BRAIN WAVES THAT ARE REFLECTIVE OF BRAIN STATE .....	72
FIGURE 6.4	A PLOT OF DETECTED EEG SIGNAL BEFORE AND AFTER APPLYING BAND PASS FILTER.....	73
FIGURE 6.5	A PLOT OF RESULTS OF THE EEG SIGNAL OBTAINED FROM THE MIMO RADAR SYSTEM.....	73

## LIST OF TABLES

---

TABLE 3.1 ELECTROMAGNETIC (EM) PROPERTIES OF HUMAN-BODY TISSUE AT 0.5 GHZ .....	40
TABLE 3.2 ELECTROMAGNETIC (EM) PROPERTIES OF HUMAN-BODY TISSUE AT 70 GHZ. ....	42
TABLE 3.3 SHOWS THE STATE-OF-THE-ART TECHNIQUES POSSIBLE FOR VITAL SIGNS MONITORING USING DOPPLER RADAR SYSTEMS. ....	48
TABLE 4.1 NORMAL ADULT’S VITAL SIGNS PARAMETERS (CLINICAL SIGNIFICANCE) .....	51
TABLE 5.1 SHOWN CLASSIFICATION OF BIOELECTRICAL SIGNALS.....	65



## LISTE DES ABRÉVIATIONS

---

SNR	Signal-to-noise to ratio
HFSS	High-Frequency Structure Simulator
ADS	Advanced Design System
CVD	Cardiovascular diseases
WHO	World Health Organization
LO	Local oscillator
EM	Electromagnetic Wave
IQ	In-phase quadrature
MIMO	Multi input Multi output
IoT	Internet of Things
ECG	Electrocardiograph
EEG	Electroencephalography
CW	Continuous-wave
FM-CW	frequency-modulated continuous-wave
RF	Radio Frequency
RR	Respiratory rate
HR	Heart rate
MPa	Pressure
SA	Sinoatrial
AV	Atrioventricular
Tx	Transmitter radar antenna
RX	Receiver radar antennas
BCI	Brain-Computer Interface

# 1 General and Definition of the Context of Research

---

## 1.1 Introduction

This chapter presents a brief introduction to non-contact and non-invasive doppler radar sensors technology. It highlights its advantages and widespread applications in the medical field. The interests and reasons that have led us to undertake this research endeavour are then expressed. Subsequently, the research objectives and challenges are concisely outlined. The main thesis contributions are listed. Finally, the thesis organization and structure are presented. Doppler Radar Sensing, a non-invasive method designed to detect vital signs of patients in health care centers, homes and disaster zones, can improve diagnosis and inform targeted treatments, a leap towards precision medicine. This work, which aspires to design and develop a medical radar sensing system, aims to increase the utilization of contactless detection and measurement of biological signals. However, widespread implementation of medical radar faces challenges including: ambiguity due to lack of range, limitations in imaging due to short observation time, and poor resistance against interferences - the prevalent signal-to-noise ratio SNR.

The aforementioned disadvantages can be circumvented by performing specific simulations and laboratory experiments. Different approaches including HFSS, MatLab, ADS, neural network models, and various algorithms are used to detect the biosignals, mainly respiration and heartbeat. Through the evaluation and integration of the said approaches, information on cardiac and respiratory from baseband signals can then be obtained with high accuracy. Quantitatively measuring the interaction between EM and the human tissues is a contributing factor to enhanced capabilities and decreased costs in the development of new antenna and radar fabrication technologies.

Using radar in medical applications as a method of monitoring inter functions and organ movement started when N. S. NAMEROW registered a patent in 1969 in the United States [74]. This technology has since evolved to detect physiological motion and health parameters. Later on, C.G. Brown Etal registered a patent in 1971 for measuring electric field radiation from living bodies [105]. The doppler radar, chosen as a model to develop these monitoring systems, allows measurements without contact with the skin by giving a faster alarm in case of human physiological and organ dysfunction i.e., vital signs. Radar-based physiology and biosignal measurement depend in part on the radar system's ability to extract valuable information about a complex structure such as the human body. In addition, the radar sensor

relies on the modulation effect of the transmitted radar electromagnetic signal when it comes into contact with the human body. Understanding of the human body's physiological functions and properties (frequency-dependent properties) as well as understanding and quantifying the interaction between the human body and electromagnetic waves is an integral part of this work. That leads to determining the optimal carrier frequency.

## **1.2 Motivation**

This thesis is a part of a large project with the goal of detecting biomechanical and directly measuring the electrical signals of living human subjects. Medical centers around the globe evidently are the mecca to people who come from distant towns seeking medical diagnosis and treatment. These patients often had to travel through difficult terrains to reach these health centres. Medical centres in underdeveloped countries are often overcrowded and rancid as many of the patients, most of the time, are old and have no family to care for them. The situation in health care centres in developed countries is not much different in the sense that vital signs are still measured manually. That often leads to a prolonged patient waiting time. Furthermore, a new study by Canadian researchers has demonstrated that long waiting times not only affect patient satisfaction, they increase the risk of death and hospital readmission for patients who have been discharged from the emergency department. In our opinion, most of the follow-up medical procedures could conveniently and easily be performed remotely using medical radar and basic “internet of things” (IoT) tools at a low cost and higher efficiency rate.

## **1.3 Research Objectives and Challenges**

The objectives and challenges of this project are to:

- Optimization of various medical radar elements to design and develop a contactless-sensing system that emphasizes high accuracy and best patients' experience.
- Study the effects of frequency, power, antenna type, polarization, body type, body position, distance between antenna and subject, signal processing techniques and antenna position on the accuracy of vital signs monitoring.
- Exploit the electromagnetic wave and human tissues interaction.
- Directly detect and measure the heart and brain electrical activities.

- Examining feasibility of using vital signs and personalized data to improve patients' experience.
- Account for ambient noise and patient sudden movement and their effect on signal acquisition and processing
- Examine and develop novel techniques, to achieve optimal frequency.

The most significant challenges in completing the project were: ambiguity due to lack of range, limitations in imaging due to short observation time, and poor resistance against interferences- the prevalent signal-to-noise to ratio SNR.

#### **1.4 Thesis Contribution**

This thesis's main contributions are listed as follows:

- Highlighting the significant discrepancies between values used in previous work and those listed in reputable medical authority's references such as the American Heart Association.
- In-depth study of EM and human tissue interaction. And integrating the results and the observations while selecting the optimal frequency to detect the respiration and heart rates.
- To the best of our knowledge, this is the first work done on directly measuring of electrical activities using multiple input multiple output radar systems.

Other contributions include:

Performed experiments on a wide range of subjects of different age, gender, health issues and more specifically heart and brain condition. That led to enhancing the integrity of our methods and results in general.

#### **1.5 Thesis Organisation**

This thesis is structured as follows:

Chapter 1 provides a general overview of radar development and medical implementation in biosignal detection. It highlights the scope and the framework of the thesis including the definition of the context of the study, motivation, contribution, objectives, challenges, and thesis organization.

Chapter 2 introduces principles and discussions on the use of the doppler radar for the detection of physiological and vital signals. It outlines the biological functions and properties of

the human body, specifically the cardiovascular activities i.e., mechanical and electrical. It presents the two categories of vital sign sensing devices i.e., contact-based and contactless based techniques.

Chapter 3 presents a comprehensive study and measurement approaches of electromagnetic waves and human tissue interaction. It introduces the architecture and operation of doppler radar and provides a list and discussion on the relevant state of the art including the limitation of previous vital signal measurement approaches.

Chapter 4 illustrates extensively the undertaken work to determine the optimal carrier frequency while measuring respiration and heart rate. This chapter also presents the use of the Advanced Design System (ADS) to perform measurement and processing of detected baseband biosignals i.e., respiration rate, heartbeat and ECG. Lab experiments at INRS and results are also presented in this chapter.

Chapter 5 performs a direct detection of the cardiac-electrical signal via MIMO radar. And it briefly touches upon the cardiac electro-mechanical signals correlation. Diagrams and graphs to illustrate the cardiac cyclic events are also presented.

Chapter 6 introduces electroencephalograph as a crucial tool in brain monitoring and brain diagnosis. A direct detection of the brain electrical signal is performed using the MIMO radar system.

Chapter 7 provides the conclusions, recommendations, and possible future work.

## 2 Principles and Implementation of Doppler Radar

---

### 2.1 Doppler Radar Based Healthcare System

A value-based healthcare system that integrates coordinated, high-quality, cost-effective, non-invasive and rapid radar sensor systems will continue to drive the design and the development of medical devices, applications and services in both traditional and telemedicine settings. Contact-free diagnosis of respiratory and cardiovascular diseases is of critical importance, especially during times of pandemics, infrastructure crises and natural disasters. Cardiovascular diseases (CVD) represent a major cause of morbidity and mortality worldwide, with estimates from the World Health Organization (WHO) global health indicating an increase in deaths from CVD from 14.2 million in 2000 to 17.9 million in 2019. The rise in CVD cases and associated mortality can be attributed to multiple factors, including an ageing population, therefore, poses a risk to healthcare systems and economies compared to other illnesses as illustrated in figure.2.1 [91]. Most of these deaths could be avoided through the continuous monitoring of vital signs since manifestation in heart and respiratory alarming signals start to be detected up to eight hours before an acute health episode [15].

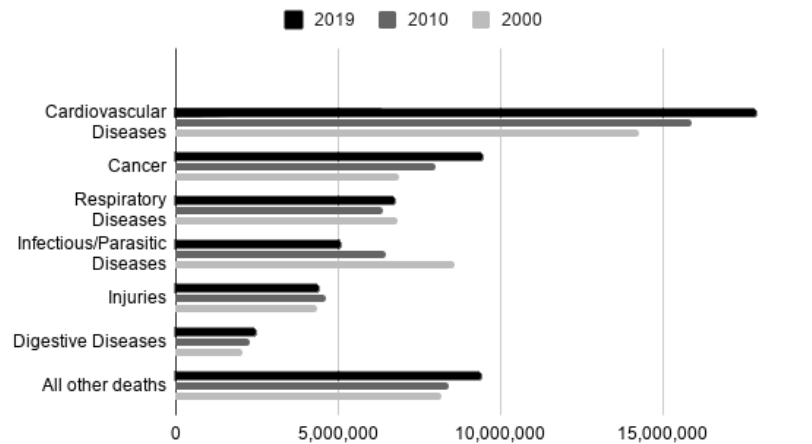


Figure 2.1 Global causes of death 2000, 2010, 2019

### 2.2 Physiology and Vital Signal Measurement Using Radar

Radar systems transmit electromagnetic or radio waves. Most objects reflect radio waves, which can be detected by radar system. The frequency of the radio waves used depends on the radar application. Radar systems are often designated by the wavelength or frequency

band in which they operate using band designations [95]. The range of the radar system is also influenced by the choice of frequency. Higher frequency systems usually are of lower power due to electronic circuit limitations and normally experience greater atmospheric attenuation [55].

A radar's ability to extract valuable information about a complex structure, such as the human body, is to a large extent technology-driven. For example, continuous-wave (CW) radars are very sensitive devices in detecting movement, such as time-varying physiological phenomena. The use of CW radar to monitor heart rate and pulmonary motion appears to be the predominant interest in medical radar during the 80s [56]. When monitoring these vital signs using traditional methods, many electrodes or terminals are placed on the body of the patients, which makes them uncomfortable. Furthermore, the traditional method is unsuitable for patients with skin abrasions and for long-term monitoring. The non-contact method has the potential to overcome these irritations with the use of radar to monitor cardiac conditions. It was first published in 1972 by Johnson and Guy [94]. A continuous-wave (CW) radar was proposed by Lee and Lin to measure the movement of the peripheral artery wall in relation to the pressure pulse wave and to extract clinical features from the signal [3].

### 2.2.1 Radar Sensor Systems

There are at least two operational modes for radar-based structural health monitoring systems: the first one is based on Doppler signatures for vibration sensing either in a continuous-wave (CW) [32], [41] or a frequency-modulated continuous-wave (FM-CW) mode [63]. Usually, most proposed Doppler radar devices that are used for monitoring vital signs consist of a microwave system operating at a single carrier frequency with a continuous wave (CW) signal excitation even though other radar schemes may also be possible. When the operating frequency increases, the wavelength decreases, and thus, the system size decreases. On the other hand, the free-space loss increases with frequency [6]. This suggests that radar presents different system behaviour at different frequency channels. Using radar in medical applications as a method of monitoring inter somatic circulatory functions and organ movement started when N. S. NAMEROW registered a patent in 1969 in the United States [74]. This technology has since evolved to detect physiological motion and health parameters. An apparatus for measuring simultaneous physiological parameters such as heart rate and respiration without physically connecting was first introduced by Steven's in 1990 [37].

Radar techniques have been considered as one promising technique in vital signs measurements. Vital signs detection with radar sensors relies on the modulation effect of the transmitted radar signal when it comes into contact with the human body. The modulation is derived from chest displacement of the human target due to both mechanical respiratory and heart electrical activity signals, along with common external noises from electronic sources and background medium conditions [28]. To improve the sensitivity of radar for vital signs detection while preserving low cost and architecture simplicity, we have proposed and investigated the use of both fundamental and harmonic components of the carrier frequency by taking advantage of the inherent nonlinearity characteristics of the mixer and other linear and nonlinear building blocks. The proposed radar can generally provide a good compromise between efficiency, compactness, and low cost. Noise and sensitivity are important and much-involved characteristics of a radar system for bio-detection and sensing because of weak and slow-paced signals, especially heartbeat signals [9].

### **2.2.2 Principles and Components of the CW Doppler Radar System**

The CW radars are the most common and simpler radar type. Several studies have already demonstrated the capacity of these radar systems in the measurement of respiratory and heartbeat signals in the microwave [38]. The CW working principle is based on the doppler effect [40]. The doppler effect occurs when there is a change in frequency in the radiated or reflected radio wave due to the movement of the object. When a continuous wave is transmitted towards an object, the reflected signal is either frequency modulated or phase-modulated [87]. The target's velocity is obtained through the difference in frequency between transmitted and reflected RF signals. For this reason, they are also known as Doppler Radar.

The velocity of the chest during the successive expansion and contraction is insignificant towards the variation of RF frequency signals. Hence the tracking of fine chest wall motion is acquired by phase shift measuring of the reflected waves over time. Thereby, the frequency of the signal is an important parameter to consider when using CW radar for vital signs sensing applications since the millimetric target chest displacement is measured over frequency and the total wavelength. In addition, higher frequencies of the carrier wave signal lead not only to higher sensitivity signals but also significant energy losses during their travel in the medium, which may guide into a detailed loss of cardiovascular signals. Therefore, a basic understanding of "medical radar" principles along with determining the optimal frequency, power, antenna design, polarization, body type, body position, antenna distance from the chest, signal processing techniques and antenna position requires

components of high technical specification. These basic principles and components play a crucial role in the accuracy of vital signs monitoring and detection. The Doppler Radar system consists of a transmitter producing electromagnetic waves in the radio or microwave domain, a transmitting antenna, and a receiving antenna. Figure 2.2 shows a block diagram of the Doppler radar system's layout for remote sensing - process and components. [34]. The setup includes three main components: (1) transmitter Tx and receiver Rx radar antennas; (2) the amplifiers, band-pass and low-pass filters and splitters; and (3) the data acquisition and signal-processing system using an oscilloscope and MatLab. The setup is configured with two In-phase and quadrature channels. Then, the arctangent demodulation was performed on these I and Q signals using the MatLab as well.

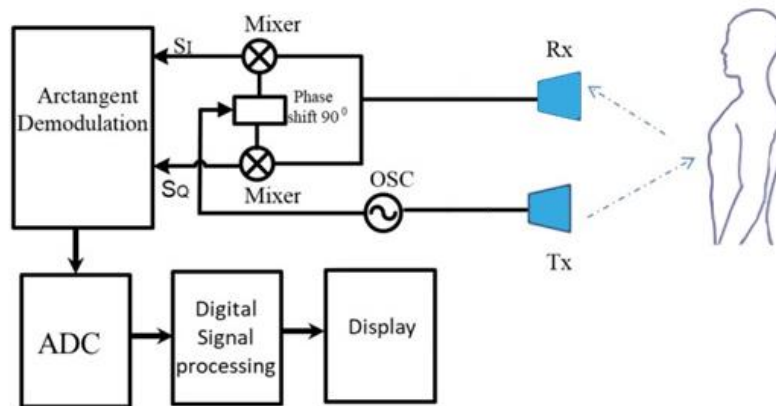


**Figure 2.2 Doppler radar operation modes used in vital signs sensing applications.**

Radar sensor modules can conveniently measure biosignals at a distance, and without the need for contact with the human body. The development of such a novel product can open doors for more research in this area and bring new opportunities to non-contact remote vital signs sensing applications. The test radar was implemented using, at times, waveguide technology which may also improve the detection of vital signs by filtering off the sub-harmonics of the radar signal [57]. The Doppler radar sensor system can be used to detect and monitor the movement of human tissues and organs without touching the body thus providing a non-invasive technique to diagnose diseases related to the heart, lungs, and vascular system [22].

### 2.2.3 Human Body Physiological Functions and Properties

The human body is a complex, highly organized structure made up of unique cells that work together to accomplish the specific functions necessary for sustaining life. The fundamental building blocks are made of elements such as oxygen, carbon, hydrogen, and nitrogen, form

the various tissues of different body systems [92]. The integumentary system is the largest organ of the body that forms a physical barrier between the external environment and the internal environment that it serves to protect and maintain. The integumentary system includes the epidermis, dermis, hypodermis, associated glands, hair, and nails [24]. The cardiovascular system is made up of the heart and blood vessels. The properties of biological tissues are wide-ranging, from cell membranes with a modulus of about  $10^{-4}$  MPa to bone with ultimate tensile strength and modulus of about 200 MPa and 15 to 20 GPa, respectively. [67].

The recent development and proliferation of electromagnetic-wave-based medical devices such as magnetic resonance imaging (MRI), and radiofrequency ablation (RFA) necessitate further research and a better understanding of the interaction between the human body and electromagnetic waves. The tissues of which the body is formed are lossy dielectrics that behave as a medium in which the electric conductivity is not equal to zero however it is not a good conductor. Such material would dissipate the energy of the electromagnetic waves propagating through it [13]. The absorptive effects of the body can then be quantified and relationships between the absorptivity of the body and its biometric parameters can be measured and studied. Measuring the effects of absorption, therefore, is essential while monitoring specific biological functions such as respiration and heart activities [93].

### **2.3 Vital Signal**

Accurate measurements of vital signs and bioelectrical signals are an integral part of any patient rescue and monitoring health system. The most common measurements of vital signs are blood pressure, body temperature, heart rate and respiratory rate. Physicians depend on these measurements to determine which treatment protocols to follow to make life-saving decisions. Monitoring of a patient's vital signs is also a crucial part of the intensive care unit, and on the wards. These measurements and assessments are the critical first step for any clinical evaluation [79]. Furthermore, the need for contact-free vital signs sensing technology, especially during pandemic situations (e.g., Covid 19, SARS, H1N1, etc.) has never been so apparent. “The New Normal” is now expected to continue to drive the development of medical radar systems. Understanding vital signs and how the human body functions serves as a prerequisite to the detection of biological and organ dysfunction and a guide to the restoration and miniatures of tissue oxygen delivery.

### 2.3.1 Respiration Rate

Respiratory rate (RR) is defined as the mean number of breaths drawn per minute, normally of 12 to 20 breaths per minute with a frequency range of 0.2 to 0.34 Hz [35]. Human respiration rate is measured when a person is at rest and involves counting the number of breaths for one minute by counting how many times the chest rises. Respiration rates may increase with fever, illness, or other medical conditions. The chest surface moves predominantly due to inflation and deflation of the lungs during the breathing cycle. This movement ranges from 4 to 12 mm [76]. Breathing or pulmonary ventilation have two phases - inspiration and expiration. It is a mechanical process that depends on volume changes in the chest cavity. The volume changes result in pressure changes, which lead to the flow of gases to equalize the pressure [84].

## 2.4 Heart Rate

The heart is a muscular organ which pumps blood through the circulation system to transport nutrients and waste products as shown in figure 2.3 [23]. It is located at the level of thoracic vertebra T5 –T8 and its average weight are between 250 and 300 g in an adult. The heart is composed of two separate main pumps which cooperate to flow the blood in the circulatory system [85]. Heart rate is the speed of the heartbeat measured by the number of contractions of the heart per minute (bpm). The American Heart Association defines the normal sinus HR as between 60 to 100 bpm. Activities that can provoke change include physical exercise, sleep, anxiety, stress, illness, and ingestion. Heart rate is a readily available vital sign that holds important prognostic information. Generally, lower HR has been associated with lower all-cause and cardiovascular mortality. It should be noted, however, that the commonly accepted heart rate norms are derived using in-clinic recorded HR. [86]. That may not be representative of the real world i.e., outside of a healthcare institution setting. However, remotely obtained measurements that are commonly recorded by a growing number of consumer devices provide a true representation of the heart rate. For example, clinic measured data can be artificially increased in a similar phenomenon to “white-coat hypertension” or by an increased adrenergic reaction to the clinical environment [46]. In addition, these measurements do not account for health status, cardiovascular fitness, gender, or racial differences [52]. Moreover, ambulatory heart rate has been found to be a stronger predictor for all-cause mortality than in-clinic resting heart rate, yet this real-world measurement is infrequently obtained [65]. The chest surface motion also includes comparatively faster but weaker vibrations (precordial motion) due to the

beating of the heart. The chest surface motion due to the beating of the heart has an amplitude range of 0.2 to 0.5 mm and a frequency range of 1 to 1.66 Hz [76].

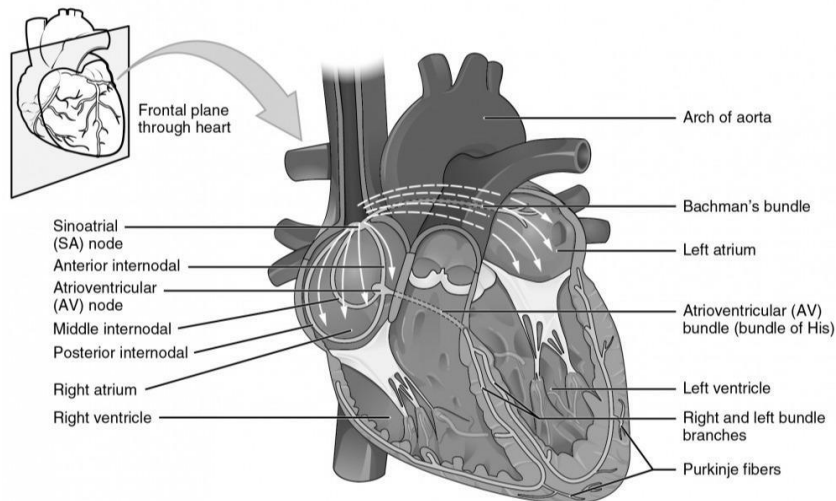


**Figure 2.3 Anterior view of the frontal section of the heart**

#### 2.4.1 Cardiovascular Activity

The cardiovascular system provides blood supply throughout the body. By responding to various stimuli, it can control the velocity and amount of blood carried through the vessels. The cardiovascular system consists of the heart, arteries, veins, and capillaries. The heart and vessels work together intricately to provide adequate blood flow to all parts of the body. The regulation of the cardiovascular system occurs via a myriad of stimuli, including changing blood volume, hormones, electrolytes, osmolarity, medications, adrenal glands, kidneys, and much more [17]. The main function of the heart is to pump blood through two circuits: 1. Pulmonary circuit: through the lungs to oxygenate the blood and remove carbon dioxide. 2. Systemic circuit: to deliver oxygen and nutrients to tissues. In order to beat, the heart needs three types of cells: 1. Rhythm generators, which produce an electrical signal (SA node) 2. Conductors to spread the pacemaker signal. 3. Contractile cells (myocardium) to mechanically pump blood. Thus, the electrical and mechanical sequence of a heartbeat [42].

The cardiac cycle describes the sequence of electrical and mechanical events that occur with every heartbeat. The normal duration of a cardiac cycle for a heart rate of 75 beats/minute is 0.8 seconds.

$$\text{Duration of the cardiac cycle (second / beats)} = \frac{60 \text{ (seconds minutes)}}{\text{Heart rate (beats minutes)}} \quad [2.1]$$

The cardiac cycle may be divided into phases in any number of methods, for instance, four phases or seven phases. In the four phases method, the opening and closing of the heart valves explain this method of the cardiac cycle. These phases are:

- Phase I: Filling period - the inlet valve is opened to fill the ventricle and the outlet valve is closed. The volume of blood in the ventricle increases from about 45 mL (from the previous cycle) to about 115 mL.
- Phase II: Period of isovolumetric contraction - both valves are closed, blood volume is constant but the blood pressure increases to about 80 mmHg.
- Phase III: Period of ejection - the outlet valve of the ventricle is opened and the inlet is closed and due to more contraction, the blood pressure rises.
- Phase IV: Period of isovolumetric relaxation - both valves are closed and intraventricular pressure decreases without any blood volume changes.

The period of relaxation is called diastole in which the ventricle fills with blood and the period of ventricular contraction is called systole. Figure 2.4 shows the cardiac cycle events for the left pump of the heart for two complete cycles [82]. This figure illustrates the pressure volume of the events. The top three curves illustrate the pressure changes in the left pump of the heart including the aorta, left ventricle and left atrium. The fourth curve from the top denotes the volume changes in the left ventricle, the fifth one is the electrocardiogram curve and the sixth curve denotes. phonocardiogram (PCG; heart sound). [85]

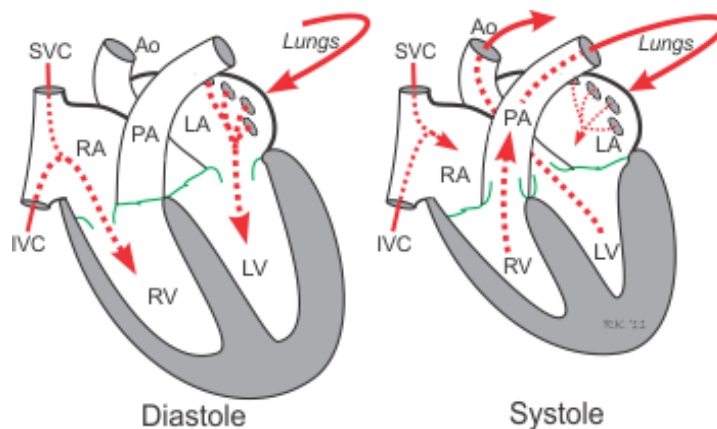


**Figure 2.4** The cardiac cycle events for the left pump of the heart for two complete cycles

#### 2.4.2 **Electrical Impulses of the Heart**

The right atrium of the heart contains the pacemaker cells [1]. These cells are directly responsible for the control of the heart rate. They generate electrical impulses that synchronize the heart beating. These impulses cause both atria to contract simultaneously. The electrical signal generated by the sinoatrial node SA node spreads to the ventricular muscle via particular conducting pathways: internodal pathways and atrial fibers, the atrioventricular node AV node, the bundle of His, the right and left bundle branches, Purkinje fibers. When the electrical signal of a depolarization reaches the contractile cells, they contract. On the other hand, when the repolarization signal reaches the myocardial cells, they relax. Thus, the electrical signals cause or interrelate to the mechanical pumping action of the heart [89]. Capturing of regular or abnormal activity of the human heart is usually done with an electrocardiogram ECG monitor device.

#### 2.4.3 **Electrocardiogram ECG**

The electrocardiogram (ECG) is a biomedical signal and a tool commonly used to monitor the electrical activity of the heart. ECG is a somewhat non-invasive diagnostic modality that has a substantial clinical impact on investigating the severity of cardiovascular diseases [11]. Metrics from ECG have been widely used for detecting heart diseases due to their simplicity and non-invasive nature. ECG is also being used for monitoring patients on antiarrhythmics and other drugs, as an integral part of preoperative assessment of patients undergoing non-cardiac surgery, and for screening individuals in high-risk occupations and those who are participating in sports [11].

Features of ECG signals can be computed from ECG samples and extracted using software programs, e.g., MATLAB, and Python [10]. The components of the ECG signal include morphological features (1) QRS complex amplitude (mV) which represents depolarization of the ventricles, (2) PR interval (ms), (3) ST interval (ms), (4) QT interval (ms), (5) P wave amplitude (mV) which represents depolarization of the atria, and the T wave, which represents repolarization of the ventricles [40]. Distinguishing the components of an ECG signal will yield more helpful information. Typically, the recording of an electrocardiogram is conducted by attaching electrodes to the patient's body, and the device will receive electrical signals from these electrodes [19]. Different types of arrhythmias or cardiovascular-related conditions are manifested in those ECG signals.

#### 2.4.4 Electroencephalography EEG

An electroencephalogram (EEG) is a recording of cerebral electrical potentials by electrodes on the scalp surface, face, and scrubbed with a conducting gel to facilitate measurement of the electrical activity of populations of neurons (scalp electrodes) and muscle activity (face electrodes). The basic methods for preparing a human participant for EEG data collection will serve as a foundation for the two Alternate protocols, which detail specific event-related potential (ERP) paradigms. [55], [88]. Electroencephalography (EEG) is therefore a possible alternative neuroimaging technique that does not possess the same limitations. The EEG has a temporal resolution in the order of a few milliseconds that makes it suitable for measuring cortical changes during workplace activities [44]. According to four kinds of typical brain EEG frequency ranges are categorized as delta (1 - 4 Hz), theta (4 - 8 Hz), alpha (8 - 13 Hz), and beta (>13 Hz). Very high frequencies (typically 30 - 40 Hz) are referred to as gamma activity. [110]. Each frequency band can be used to describe the mental state of a person. Alpha and beta frequency power is linked to negative mood, stress and depression. Furthermore, the electroencephalogram as a diagnostic technique can be further extended to measure cardiovascular activity since the electrical system is affected by neurotransmitters from the brain. [44]

### 2.5 Devices and Techniques Used in Measuring Biosignal

Sensing vital signs can be categorized into contact-based techniques and contactless based techniques. Conventional clinical methods of detecting these vital signs require the use of contact sensors, which may not be particularly practical for long-duration monitoring and less convenient for repeatable measurements. On the other hand, wireless vital signs detection using radars has the distinct advantage of not requiring the attachment of electrodes to the subject's body and hence not constraining the movement of the person and eliminating the possibility of skin irritation and other inconvenience added to the patient experience. In addition, it removes the need for wires and limitations of access to patients, especially children and the elderly [16].

#### 2.5.1 Implantable Sensor (Invasive Techniques)

Traditional methods of detecting vital signs leverage on contact sensors, which are impractical for long-term monitoring and inconvenient for repeatable measurements. These contact sensors are mainly wearing devices such as electronic bracelets and chest-wearing receivers,

in which the electric current is generated by direct contact between the electrode pad and the skin to monitor the characteristics of respiratory and heart rate after passing through the body. Unfortunately, most of these contact vital signs monitoring devices are of poor performance and bring an irritating effect on the user [53]. The pulse oximeter and the electrocardiogram are contacting sensing devices commonly used in hospitals to monitor the heartbeat of patients. In most cases, breathing rate-monitoring techniques require contact between the person and the equipment like an electrocardiogram, stethoscope, oximeter, or phonocardiogram.

Figure 2.5 [48]. Illustrates the traditional ECG measurement techniques that can only be performed in a hospital environment, where specific equipment and various wired direct-skin-contact electrodes are needed. That is not appropriate for long-term daily-life ECG monitoring due to the imposed skin irritation, movement artifacts, and daily-life disturbances induced by the wired electrodes [64]. The same measurement approach disadvantages, with probably more irritation and inconvenience, applies to traditional EEG measurement as shown in figure 2.6 [90].

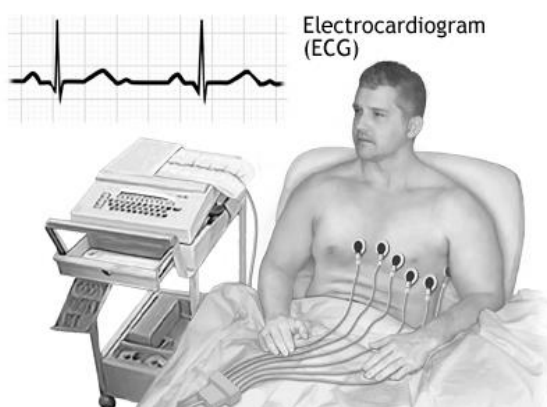


Figure 2.5 The traditional ECG measurement



Figure 2.6 EEG device measurements

### 2.5.2 Non-invasive Techniques

A non-invasive method i.e., contactless measurement of vital signs complemented with utilising IT and internet of things IoT technology opened a new door to the field of telemedicine. Non-contact detection and monitoring of vital signs have significant importance

in several scenarios [48]. The detection of life after avalanches or earthquakes, senior care at home, the monitoring of sleep, and the care of patients that cannot use contact devices, and so forth. In addition to optical techniques such as photoplethysmography. There are many advantages of using the non-invasive technique over the use of traditional contact techniques. Advantages in terms of cost, efficiency, time, accuracy, practicality and reliability. In addition, these techniques offer convenience and better patient experience, especially at times of health concerns during epidemics. It also reduces the concern of white-coat hypertension and irritation to people with special needs [98].

### 3 Study of Electromagnetic Waves and Human Tissues Interaction

---

#### 3.1 Interaction of Electromagnetic Radiation with the Human Body

Electromagnetic wave impulses are able to propagate through the human body. Figure 3.1 shows normal electromagnetic wave propagation. Different layer's interface of human tissues has different reflection magnitudes. Several works in literature that are interested in estimating the scattering of electromagnetic waves by the human body [49]. The interaction of electromagnetic waves (EM) with the human body is a complex function of numerous parameters. The proliferation of electrical technologies raised new areas for study, including the analysis of the interaction of electromagnetic radiation with the body's lossy dielectrics tissues. Since the body's tissues possess a range of dielectric properties such as conductivity, permittivity and penetration, knowledge of these properties and their interaction with electromagnetic waves and its propagation is necessary when designing medical applications and devices [50].

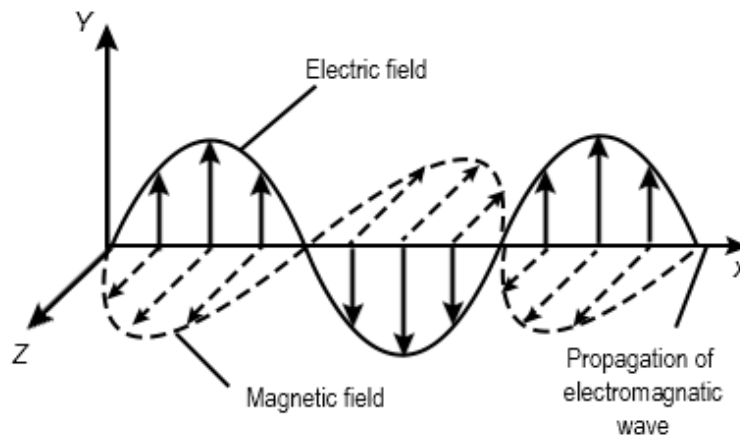


Figure 3.1 Shown propagation of electromagnetic wave

There is a wide range of electrical properties which control propagation, reflection, attenuation, and other behaviour of electromagnetic fields in the body. These attributes depend strongly mainly on the tissue type and the frequency of interest. The need for extensive data on the dielectric properties of human tissues is often and strongly felt among scientists and researchers involved in the understating of the interactions of electromagnetic (EM) fields and biological systems [51]. The composition and properties of the human body are highly inhomogeneous. Bone, blood, muscle, etc.; all have different permittivities and conductivities.

Since the permittivity of human tissue is frequency dispersive, it is important to understand these frequency-dependent properties. [77].

Schwan, Foster, Stuchly, Gabriel, and others performed studies on the dielectric properties of human tissues. Gabriel's results are summarized in a database. Typical results are displayed in figure 3.2. The behaviour of the conductivity from low frequency to 20 GHz is as follows: below 200 MHz the conductivity is relatively flat, but it increases almost linearly at higher frequencies up to about 20 GHz and then the slope decreases. This is due to the transition from dc conductivity to dielectric relaxation. In fact, the body is a complicated mixture of organs and materials with widely varying dielectric properties. [97].

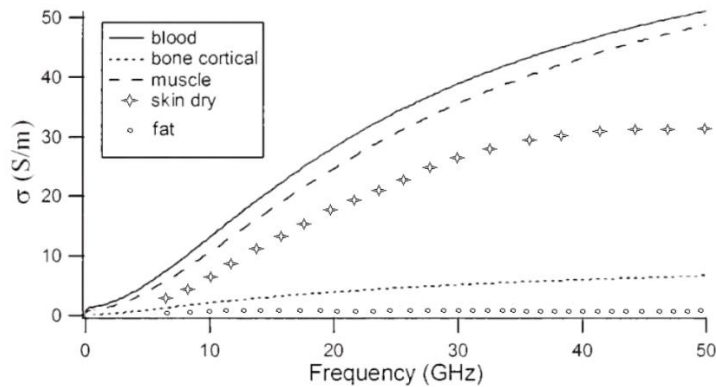


Figure 3.2. Measurements of the conductivity (S/m) of various body tissues by Gabriel and Gestblom

### 3.2 Simulation and Measurement of Body Tissues and EM Interaction

The aim of this subsection is to study the interaction of EM and human tissues. And to quantify the absorption of EM in order to enhance the accuracy of detecting vital signs and the overall spectral analysis. Several carrier frequencies were used ranging from 0.5 to 70 GHz. Modelling of body tissue and EM wave interaction was done using Ansys HFSS simulation software. The scattering of EM is characterized and measured through frequency-dependent parameters such as permittivity, conductivity and penetration. Previous work showed penetration, in millimetres, of different tissues at different frequencies i.e., lung 85mm, muscle 35mm, fat 5mm, skin 5mm. By piecing together, the data available, the main features of the dielectric spectrum of biological tissue are revealed. However, the said work exposed variability between data from different studies and gaps in our knowledge with respect to certain tissue types and with respect to certain frequencies. Values of frequency-dependent parameters are listed in the Gabriel & Gabriel database. [71], [14].

Table 3.1 and 3.2 list values of various frequency-dependent parameters i.e., conductivity, permittivity, loss tangent, and penetration/depth of different body tissues at both low, 0.5 GHz, and high frequencies 70 GHz. C.Gabriel resource is used to calculate the dielectric properties of body tissues. Figures 3.3, and 3.4 show a graph of measurement of the permittivity ( $\epsilon$ ) of various body tissues at different frequencies, and a graph of measurement of loss tangent of various body tissues at different frequencies respectively. They basically depict the relationship between permittivity and frequency and loss of tangent and frequency of various body tissues. It is apparent that as frequency increases, penetration decreases in all body tissues.

**Table 3.1 Electromagnetic (EM) properties of human-body tissue at 0.5 GHz.**

<b>Tissue Name</b>	<b>Conductivity [S/m]</b>	<b>Relative Permittivity</b>	<b>Loss Tangent</b>	<b>Wavelength [m]</b>	<b>Penetration Depth [m]</b>	<b>Thickness (Cm)</b>
<b>Skin Dry</b>	0.7284	44.915	0.58303	0.086137	0.050732	0.2
<b>Fat</b>	0.042793	5.5444	0.27748	0.25227	0.29486	0.96
<b>Muscle</b>	0.82245	56.445	0.52383	0.077352	0.050033	1.35
<b>LungInflated</b>	0.39101	23.207	0.60573	0.11951	0.068115	0.58
<b>Heart</b>	1.02	64.039	0.5726	0.072225	0.043208	1.3

Various factors determine the scattering of EM waves as an incident wave is reflected or propagated through a human body. Factors such as, body shape, size, geometry, posture and various dielectric properties. For the purpose of this research, we focused only on the dielectric properties.

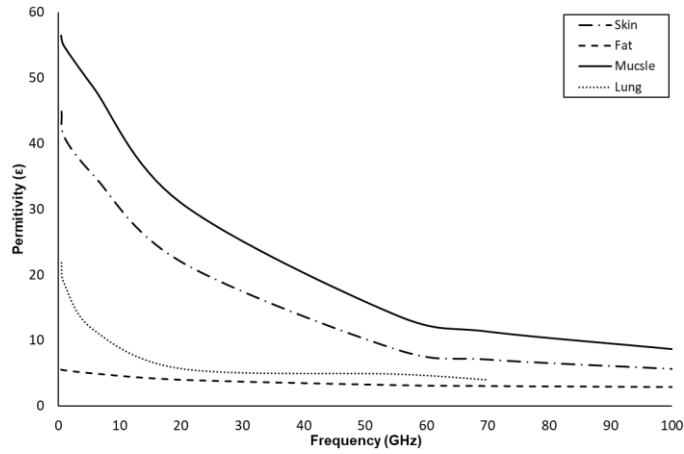


Figure 3.3. Measurement and graph of the permittivity ( $\epsilon$ ) of various body tissues at different frequencies

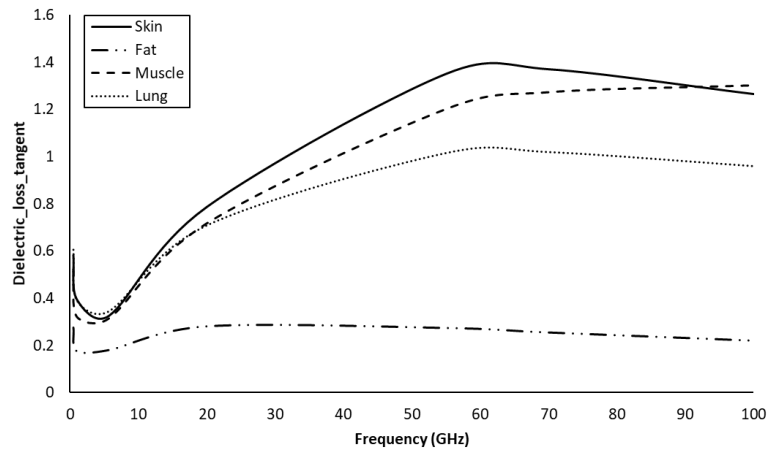


Figure 3.4 Measurement and graph of the dielectric loss tangent of various body tissues at different frequencies

Table 3.2 Electromagnetic (EM) properties of human-body tissue at 70 GHz.

Tissue Name	Conductivity [S/m]	Relative Permittivity	Loss Tangent	Wavelength [m]	Penetration Depth [m]	Thickness (Cm)
Skin Dry	37.577	7.0383	1.371	0.0013902	0.00043524	0.2
Fat	3.0436	3.0477	0.25645	0.0024336	0.0030696	0.96
Muscle	56.036	11.308	1.2725	0.0011131	0.00036452	1.35
LungInflated	19.344	4.8697	1.02	0.0017613	0.00066735	0.58
Heart	54.165	10.664	1.3043	0.0011407	0.00036797	1.3

The frequency Dependent Attenuation of the EM Radiation on biological tissues is illustrated in figure 3.5. Multilayered flat tissue model (a) and model (b) predicted attenuation of pulse-echo intensity travelling from the transmitting antenna to the receiving antenna. Each step accounts for echo at the boundary. Decreasing of the curve accounts for linear attenuation in the tissue, as shown [59].

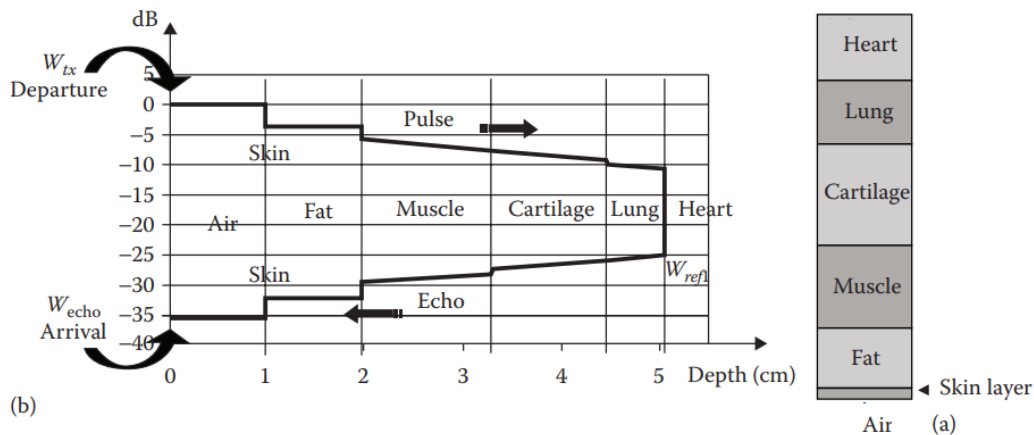
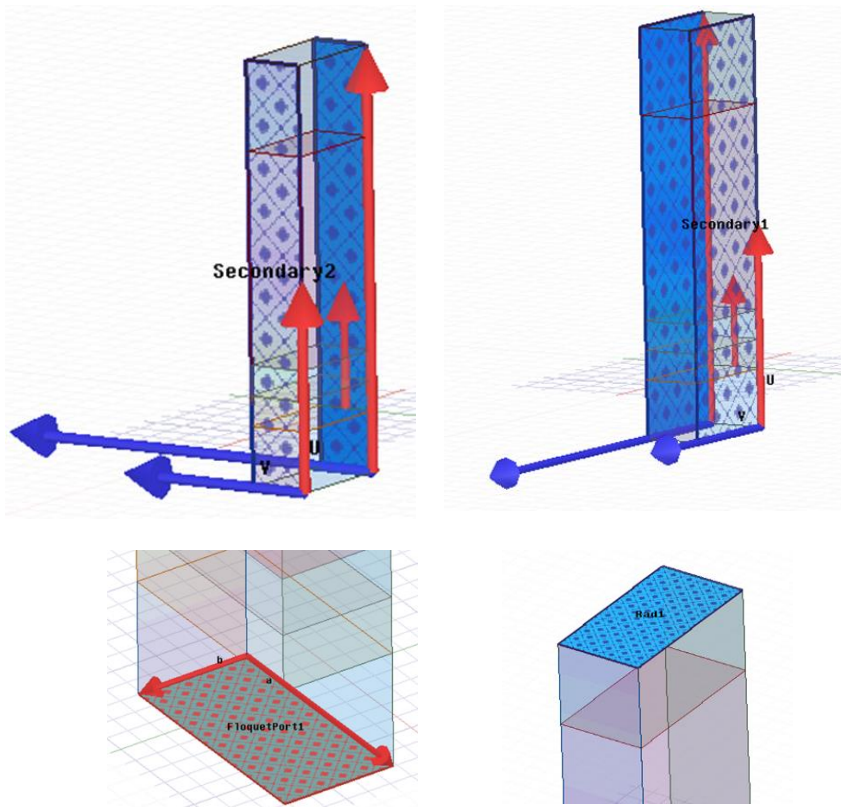


Figure 3.5. (a) Multilayered flat tissue model and (b) model predicted attenuation of pulse-echo intensity

An experimental study based on modern swept-frequency techniques may therefore consolidate our knowledge in this field. Several different runs at frequencies of 0.5, 1, 5.7, 20 and 70 GHz were performed. Furthermore, the following steps were devised to accurately extract the material parameters in order to facilitate and simplify the design procedure of the

dielectric material structures while using the simulation software: Floquet\* Port and boundary is used, each two sides of the box are paired with master and slave boundary conditions. The top side is considered as open, as illustrated in figure 3.6.



**Figure 3.6.** illustrated two sides of the box are paired with master and slave boundary conditions and the top side is considered as open.

Frequency-dependent dielectric property and penetration depth of human tissue have already been studied. Due to the complexity of the targeted human body's non-homogeneous composition; skin, tissues, fat, muscles...etc., the incident wave has not exhibited a linear propagation, especially at higher frequencies. In general, however, as frequency increases the skin/depth penetration decreases. We can conclude that at lower frequencies i.e., high penetration we can expect to capture waves reflected from inner organs. At higher frequency however, when about 72% or more of the incident EM wave is reflected by the body surface, no signal from the body's inner organs was detected; as predicted [70]. Most of the incident

wave was reflected at the outer surface. The reflection from the body and level of EM energy penetration into the human body for the said different frequencies exhibited in different colours as illustrated in figure 3.7.

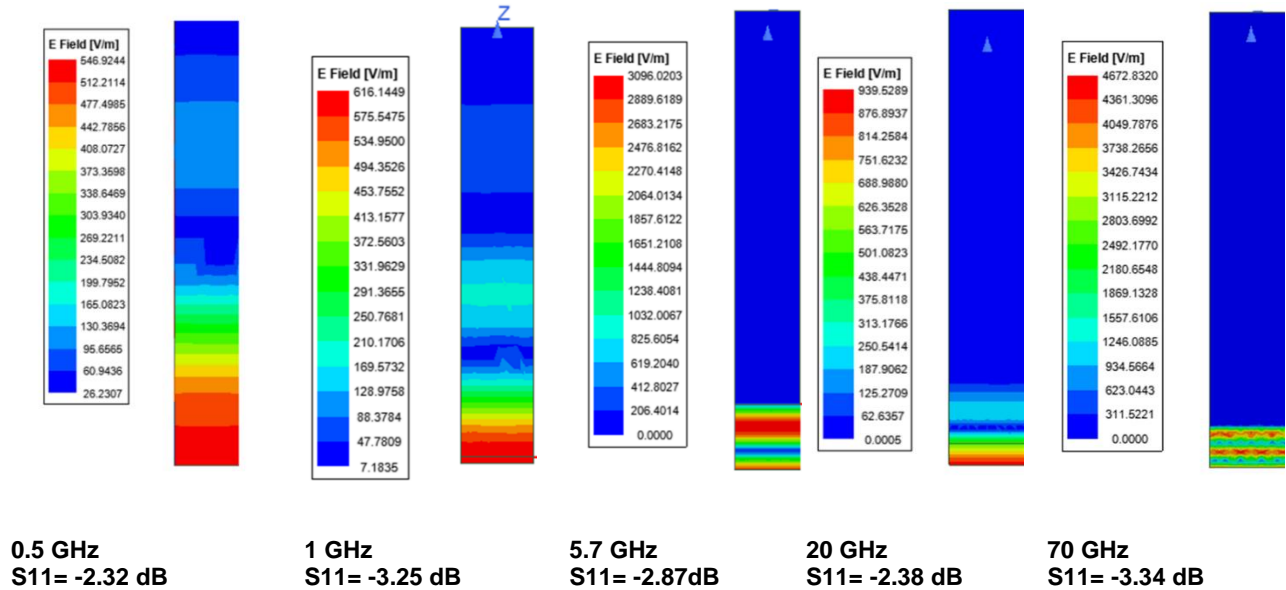


Figure 3.7 Magnitudes of penetration and reflection of electromagnetic waves through the human body.

### 3.3 Doppler Radar and the Optimization of Healthcare

Microwave Doppler radar is an extremely promising tool for monitoring the heart and breathing rate of patients with heart-related illnesses, lung disorders, diabetes etc. [53]. As previously stated, the continuously attached and invasive nature of commercial vital sign monitors is off-putting to many patients. Doppler radar can be used to monitor vital signs in a completely non-invasive way. This will greatly improve the quality of care and mobility hence improving patient's experience. Long-term monitoring will especially become more feasible due to stringent requirements by the health regulators. Such requirements render the Doppler radar ideal for a wide range of medical and research applications. The Doppler radar can measure heart rate up to a distance of 2m, [54]. Thus, it can be used as surveillance device to detect people behind walls, especially in emergency situations, such as earthquakes and other human and natural disasters. It can also be used to observe abnormal heart rates in red zones. Long route truck driver's heart rates can be tracked to detect signs of inability to drive

properly for long periods of time. The heart rate of essential service providers such as doctors, nurses, police officers, firemen, and other security personnel can effortlessly be monitored and assessed. Furthermore, it offers health care providers the advantage of detecting to detect vital signs at a fraction of the cost of high-end traditional systems. Radar systems are very-desired candidates for contactless vital-sign-monitoring applications due to their unique features to detect small vibrations [58]. With all the said advantages, employing radar sensing systems comes with a number of challenges. The chief of which is poor resistance to interferences or signal-to-noise ratio SNR.

### **3.4 Noise and Radar Sensing**

Noise radar technology (NRT) is based on the transmission of random waveforms as opposed to the classical, often sophisticated, deterministic radar signals. Both NRT and “deterministic radar” technology use the “matched filter”, or an approximation of it, to maximize the signal-to-noise ratio (SNR). In a conventional radar, a single waveform (or a finite set of waveforms), is used for transmission and reception with matched filtering. Conversely, NRT is able to transmit a—virtually unlimited—set of realizations (i.e., “sample functions”) of a random process, with the pertaining matched filter set up in real time to implement the well-known “correlation receiver” [101].

In continuous wave doppler radar, there are two antennas as shown in figure 3.8. [102]. One is constantly transmitting while the other one is constantly receiving. Although CW doppler radar has the advantage of high sensitivity and can detect small doppler shifts, the encountered noises overlap with an already complex signal reflected from the target. The signal received from the subject, due to chest movement, and other surrounding noises have many doppler shifted frequencies. Spectral analysis is then performed to extract the individual component frequencies from a complex spectrum of signals [56]. The extracted signals contain information on respiration rate, heart periodic movement, and electrical activity. Vital signs and heart conditions can then be determined using an array of signal processing techniques [57]. Medical radar sensitivity to noise reduces signal quality even at slight body movements. Previous studies have shown that the vital sign detection algorithm may not be accurate in the presence of body movements in the signal. A mismatch between the RR and HR extracted from radar and reference signals occur when there is a body movement [39].

### 3.5 Architecture and Operation of CW Doppler Radar

A typical architecture of quadrature continuous-wave Doppler radar is shown in figure 3.8. The radar transmits sinusoidal electromagnetic waves generated in the local oscillator (LO) which are then amplified in the power amplifier (PA). The transmitted signal, upon hitting the human subject, modulates the amplitude of the heart and respiration signals then is reflected back. The transmitted signal can be expressed as shown in equation 3.1.

$$T(t) = A_t \cos[2\pi f t + \phi(t)], \quad [3.1]$$

where  $A_t$  and  $f$  are the amplitude and the frequency of the transmitted signal respectively, and  $\phi(t)$  is the phase noise of the local oscillator. The received signal  $R(t)$  after a round trip delay can be written as 3.2.

$$R(t) \approx \text{Arcos} \left[ 2\pi f t - \frac{4\pi d_0}{\lambda} - \frac{4\pi x(t)}{\lambda} + \phi \left( t - \frac{2d_0}{c} \right) \right] \quad [3.2]$$

where  $T_t$  is the transmitted signal and  $\phi$  is the arbitrary phase shift or the phase noise of the signal source. The reflected signal  $R_t$  is influenced by the movement of the abdomen during respiration, at a nominal distance  $d_0$ . The reflected/received signal  $R(t)$  accounting for the phase shift is expressed as shown in equation 3.3 below:

$$R_t \approx \text{Arcos}[2\pi f t - 4\pi d_0/\lambda - 4\pi x(t)/\lambda + \phi(t - 2d_0/c)] \quad [3.3]$$

The oscillatory body displacement due to heartbeat ( $m_h$ ) and respiration ( $m_r$ ) can be expressed as: 3.4,3.5

$$x_h(t) = m_h \cdot \sin \omega_h t \quad [3.4]$$

$$x_r(t) = m_r \cdot \sin \omega_r t \quad [3.5]$$

The resulting baseband signal equation is written as equations (3.6,3.7):

$$B(t) \approx \text{COS} \left[ \frac{4\pi x h(t)}{\lambda} + \frac{4\pi x r(t)}{\lambda} + \emptyset \right] \quad [3.6]$$

$$= \sum_{k=-\infty}^{\infty} \sum_{i=-\infty}^{\infty} J \left( \frac{4\pi x h}{\lambda} \right) J_k \left( \frac{4\pi x r}{\lambda} \right) \text{COS}(K\omega r t + l\omega h t + \emptyset) \quad [3.7]$$

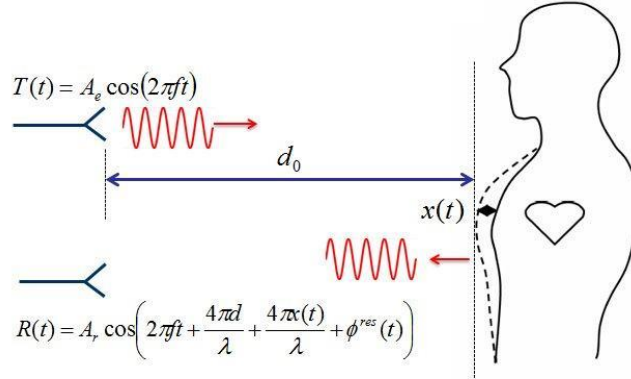


**Figure 3.8. A simplified block diagram of Doppler-radar based vital signs monitoring. The tracking of fine chest wall motion can be obtained by measuring the phase shift of the reflected signals of continuous-wave radars. The higher the frequency of the transmitted radar signal, the higher sensitivity.**

Doppler radars transmit a signal of a continuous-wave (CW) tone. The received echo is mixed with a replica of the transmitted signal, leading to the in-phase and quadrature (I/Q) components of the baseband signal, whose phase is related to the vital signs. Since the first application of Doppler radars to monitor vital signs of animals, many efforts have been devoted to improving their architecture. For example, DC-coupled schemes have been investigated to avoid distortion of the low-frequency components of the vital signs and low-intermediate-frequency (low-IF) solutions have been approached to circumvent issues regarding undesired flicker noise and saturating DC offsets [43].

### 3.6 Relevant State of the Art

Various approaches and techniques of using doppler radar have been used by many researchers to detect vital signs. The aforementioned techniques can be classified under two categories. The first focuses on the interaction of EM waves with the human body. The second puts more emphasis on signal processing and analysis. The latter being the more common approach as shown in more details in table 3.3.

**Table 3.3. shows the state-of-the-art techniques possible for vital signs monitoring using Doppler Radar systems.**

Ref. No.	Frequency (GHz)	Power	Range	Distance	Type of Antenna	Type of Radar	Technique
[45]	0.915 2.45	-3.9 dB -4 dB	12dBm	0.80	fractal-slot patch	CW	Fast Fourier transform and digital filtering using raw signals.
[106]	5.8	11-19 dBm	-	1-1.5	patch	CW	The Time-window-variation technique
[99]	5.8	5 dBm	-	1.5	series-fed arrays	FMCW	A new compact X-band FMCW Radar
[2]	9.6	25 mW	-	2.5	patch	FMCW	Conventional signal processing techniques.
[29]	14	10dBm	16 dBi	5	-	CW	Heterodyne structure and leakage cancellation technique
[31]	24	-	-	1.5	a series-fed	CW	Advanced Radar.
[66]	24	10 dBm	-	0.75	-	CW	Artificial neural network (ANN).
[73]	24 24.5	15dBm	-	0.40	-	FMCW	A novel method using a modified waveform.
[33]	35	-	17.1 dBi	1.5	series-fed antenna array	Doppler	-
[24]	40	14dBm	20 dB	0.25	-	Doppler	A Synchronized Motion Technique (SMT).
[54]	60	-	-	2	Horn	Doppler	Artificial neural network (ANN).
[44]	77	-	-	70-90	-	FMCW	(CS-OMP) and (RA-DWT) algorithms.
[68]	80	0.5 mW	-	1 2	Teflon antenna	FMCW	The performance of an ultra-wideband FMCW-radar for vital sign detection.
[83]	76-81	10 dBm	-	≈ 1	pattern	FMCW	Range-gating and beamforming techniques.
[107]	120	-3 dBm	-	1.5	narrow beam lens	FMCW	Using narrow beam millimeter wave radar.

Evaluating previous work done on measuring human vital signs entails presenting and discussing researchers' approaches towards a number of parameters such as carrier

frequency, range and target orientation, and EM and human tissues interaction to name just a few. The integrity of a prototype or a proposed detecting system depends on or can be determined by comparing the results of the proposed system with that of standardized measuring devices and well-archived data preferably with a minimal error margin. Various considerations were taken in choosing the optimal frequency. For example, a path-loss calculation based on the simplified layer model indicates that the reflected power of a lower frequency is greater than that of a higher frequency radar [45]. Performances of the different systems are compared and studied. It showed that the highest sensitivity detection can be achieved at a frequency of 35 GHz [33]. The frequencies proposed in previous works range from 0.915-MHz to 120 GHz. Example frequency values in the literature in the lower range include 5.8GHz [106], [99], and 14GHz in [29] and higher carrier frequencies 77 GHz and 120 GHz [44],[107] respectively.

A more comprehensive study of the electromagnetic properties of biological layers is important in using radar for contactless measurements of the human heartbeat and respiration rate. Any discussion of an antenna design without investigating the interaction of electromagnetic radiation with human tissues remains incomplete. In reviewing many proposed radar systems, it's very evident that not much attention has been given to the actual physical causes of detected vital signals which could potentially open the new fields of radar-based applications in remote sensing systems design.

Experiments results show that changing body orientation, measuring from the back, for example, can effectively improve the heartbeat-to-respiration ratio (HRR) up to 76 % while the subject kept normal breathing [24]. A statistical analysis of the measured data on the different subjects and orientations was performed, showing that the radar was able to measure with high accuracy both the respiratory rate and the heartbeat in all considered configurations. The signal processing technique is of critical importance. This section provides an overview of signal processing techniques employed by previous work listed in Table [2]. The aforementioned techniques can be classified into three major categories. First, how a signal is sampled; most of the previous studies use long-period time windows to guarantee a sufficient frequency spectrum resolution for HR measurement using the peak searching method on the frequency spectrum [106]. Second, even though there is a shift away from relying on hardware, however, a compact 24-GHz radar transceiver chip, transmitting and receiving antennas, baseband circuits, microcontrollers, and Bluetooth transmission modules have been integrated and implemented on a printed circuit board [31]. A new compact X-band FMCW

radar has been built at TNO laboratories and experimental results are presented here, which demonstrate the ability of this new system to detect life-sign. [99]. Third, the algorithm employed most frequently is Fast Fourier Transform FFT and digital filtering [45], [14] a 10-s sliding-time-window FFT method, the proposed method achieves the smallest average error among the three techniques [106].

### 3.7 Limitation of Pervious Vital Signal Measurement Approaches.

In general, most of the previous works use four or five human subjects, most of the time with normal heart conditions. This approach ignores or does not account for a wide range of archived data of subjects of different ages, gender, health issues and more specifically heart conditions. Experimenting or working with small and conditioned samples hinders the integrity of the methods and the results in general. Illustration in figure 3.9. Clearly indicates that while the heartbeat amplitude is inversely proportional to the respiration strength, the amplitude of the motion induced by both respiration and heartbeat is directly proportional to the carrier frequency [20]. Visualization of the carrier frequency as a function of the ranges of the respiration-induced and the heartbeat-induced body movement, suggests that the optimal carrier frequency falls in the 0 GHz to 120 GHz frequency band.

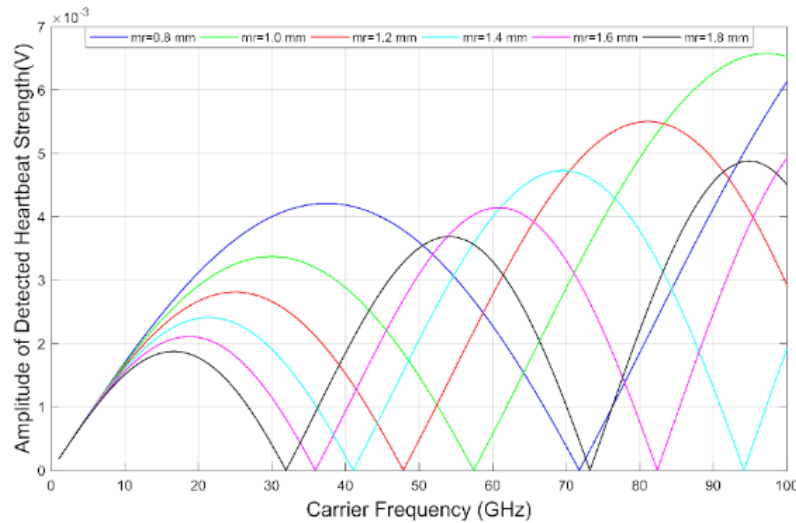


Figure 3.9 Amplitude of detected heartbeat signal vs carrier frequency

## 4 Determining the Optimal Carrier Frequency to Detect RR and HR

---

### 4.1 Optimal Frequency Measurement

We used MatLab code to simulate the measurement of vital signs i.e., heart rate and respiration rate. The measurement of the biosignals is performed while determining the optimal carrier frequency. Table 4.1 lists standard breathing rate ( $m_r$ ), heartbeat ( $m_h$ ). It must be noted that there are significant discrepancies between values used in previous works and those listed in reputable medical authorities' references such as the American Heart Association. Figures 4.1, and 4.2 illustrates the carrier frequency as a function of the detected heartbeat amplitude. As the frequency increases the detected heartbeat amplitude increases hence amplitude and frequency are directly proportional. However, at certain frequency ranges this relation does not hold and it can be characterized as being nonlinear. Also, we can see that as the respiration rate increases the heartbeat amplitude starts to decrease at a given frequency. Therefore, respiration and heartbeat amplitude are inversely proportional.

**Table 4.1 Normal adult's vital signs parameters (Clinical Significance)**

Vital Signs	Rate per min	Frequency (Hz)	Amplitude Front side (mm)	Amplitude Backside (mm)
Breathing ( $m_r$ )	12-20	0.2-0.34	4-12	0.1-0.5
Heartbeat ( $m_h$ )	60-100	1-1.66	0.2-0.5	0.01-0.2

Figures 4.1, and 4.2 also show that there is an optimal carrier frequency at each maximum detected heartbeat amplitude at a given  $m_r$ . Therefore, the respiration rate  $m_r$ , as a function of  $m_h$ , can be considered a limiting factor in determining the optimal carrier frequency. A strong heart rate signal resolution is achieved at a higher carrier frequency and at the lowest breathing rate. However, it's recommended to limit the carrier frequency to the lowest possible region. Furthermore, it's important to cover all the normal breathing rate ranges, as given in table 4.1 which can only be achieved at low carrier frequency ranges. Therefore, to maximize the amplitude of the heartbeat signal, an optimum carrier frequency is chosen for a given value of respiration  $m_r$ . The optimum carrier frequency for  $m_r = 4$  mm for example is approximately 10GHz. The optimal carrier frequency is higher for a smaller range of breathing displacement induced by  $m_r$ . The optimal carrier frequency for  $m_r$  at 10mm to give another

example is 5 GHz. It is recommended to limit the frequency of the carrier in the region below the Ka-band.

To further illustrate the effect of respiration ( $m_r$ ) interference on the detection of heart rate  $m_h$ , we performed a second experiment from the backside. The comparison between the measurement of heart rate from the front and the backside is shown below. The amplitude of the detected heartbeat signal from the backside is much higher than when measured from the front side. That clearly indicates less interference from respiration and its harmonic on heartbeat signals as we measure from the backside. The optimal carrier frequency for a given  $m_r$  could be higher if the detection is done from the back.

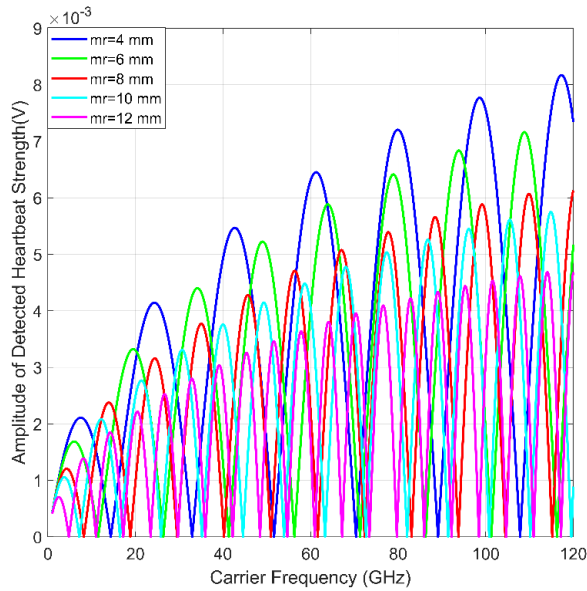


**Figure 4.1. Amplitude of detected heartbeat signal from the front side.**

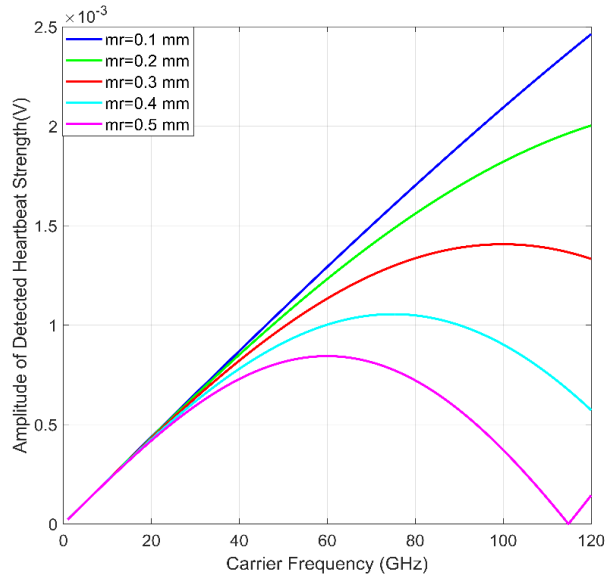
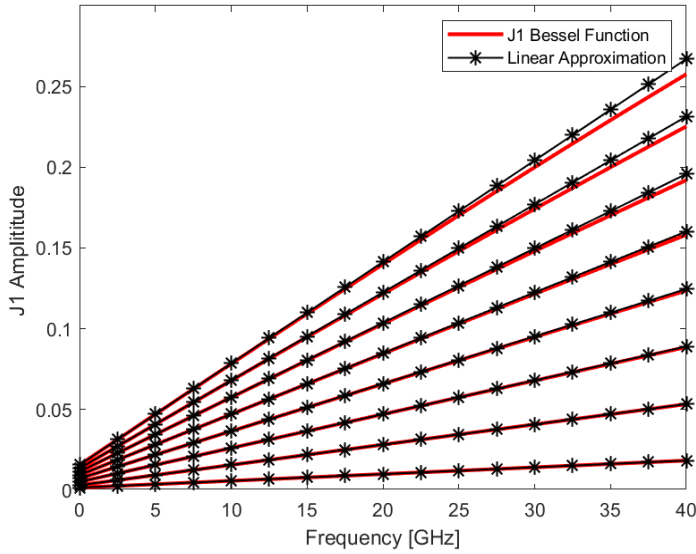
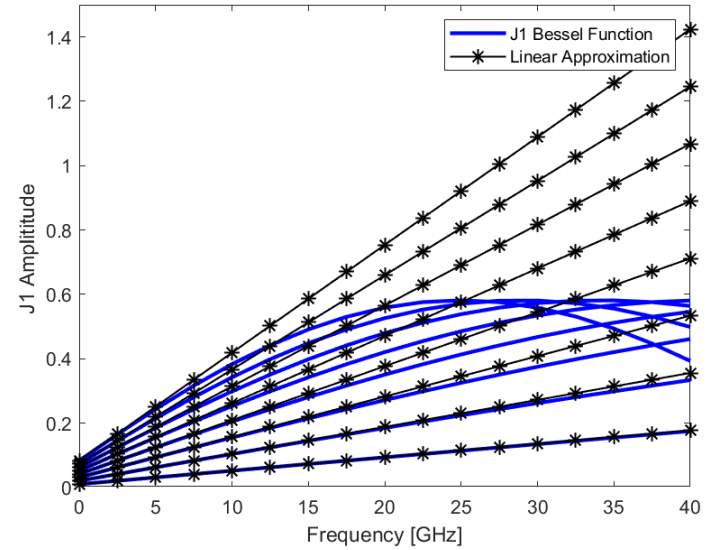


**Figure 4.2 Amplitude of detected heartbeat signal the back side.**

Figure 4.3 shows the comparison between the original Bessel function of the first kind and its linear approximation for (a) heartbeat, and (b) respiration. However, for respiration, the movement amplitude  $m_r$  is large compared to the wavelength  $\lambda$ . The approximation does not provide good accuracy, as shown in Figure 4.3 b.



(a) heartbeat



(b) respiration

Figure 4.3. Comparison between the Bessel function of the first kind of order 1 and the linear approximation for the movement amplitude cases of (a) heartbeat; (b) respiration.

## 4.2 Detection of Heartbeat and Respiration Using ADS

Radar is used to detect a subject's heartbeats and respiration contactlessly from a distance, [75] or by placing an antenna on the person's chest or back. Contactless monitoring of heartbeats and respiration can be useful in long-term vital signs monitoring. In this section we used Advanced Design System (ADS) to perform measurement and processing of detected baseband biosignals i.e., respiration rate, heart rate and ECG. Figure 4.4 shows a schematic diagram of the said system modeling the mechanism of Doppler Radar based vital sign detection in ADS.

The baseband signal can be processed further by appropriate signal processing techniques. The simulation of the proposed system is performed with ADS 2020. The human heartbeat and respiration are modelled using two sinusoidal sources with stipulated frequencies. These sources along with the phase modulator represent the human subject. Concurrent dual 7 GHz band subsystems, used by the RF system, are a microstrip patch antenna, a power combiner, and a bandpass filter. At the down-conversion section, wideband mixers with an intermediate frequency (IF) of 300-MHz are used to obtain the baseband signal. The baseband signal, obtained after the mixer stage from the simulation of the proposed system, suffers from the

DC offset. The problem of dc offset is solved by adding a capacitor at the output. That yielded a signal proportional to each of the target distance.

To demonstrate the effects of intermodulation and harmonics, the mechanism of Doppler radar vital sign detection is modelled in ADS is shown. The phase shift  $\theta$  in (1) and (2) is realized by a phase shifter, labelled as PS, and the body movement caused by respiration and heartbeat is modelled by two cascaded sinusoidal signal sources SRC1 and SRC2. As both the double-sideband transmission and the quadrature transmission are able to reduce the null point problem in vital sign detection, quadrature architecture is chosen here for the ease of simulation. Moreover, the simulation results presented in the following were obtained in the case when both of the two quadrature channels are in the middle between the null point and the optimum point.

This section presents measurements and analyses performed using ADS. Figure 4.4 shows the schematic of the radar used in our simulation. We consider that the radar transmits a continuous-wave (CW) signal at a given frequency. This transmitted signal passes through the free space and is then modulated in phase by the vital signals (respiration, heartbeat, ECG) model. One main scenario is considered in our experimentation. In this single-target experiment, the RR and HR of the person is estimated when the subject is located at a fixed distance from the radar system.

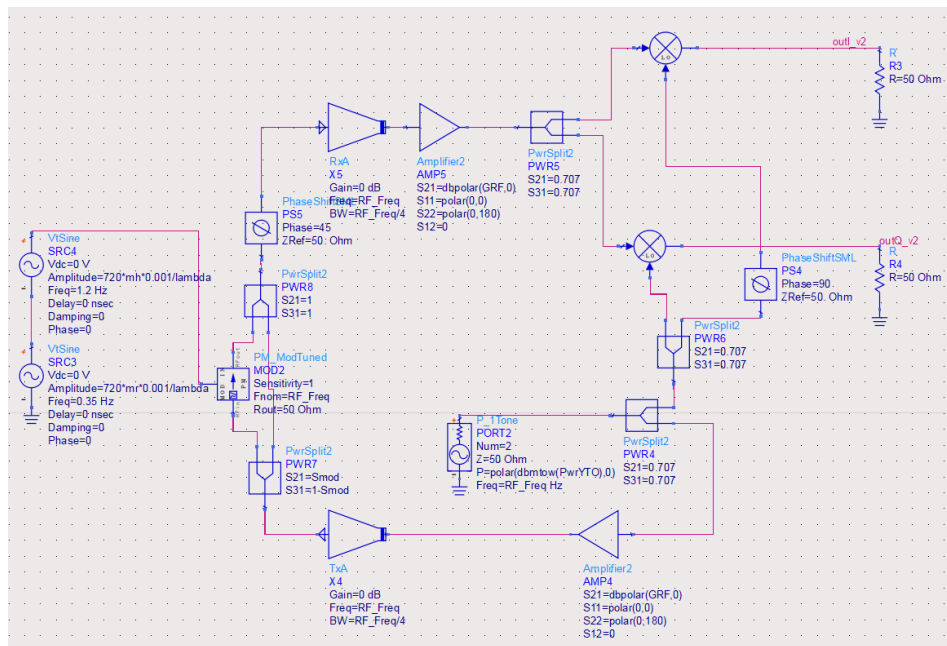


Figure 4.4 An ADS schematic diagram of Doppler Radar systems to simulate the detection of biosignals

Figure 4.5 (a) shows the raw signals of doppler radar vital signs i.e. respiration and heartbeat. As shown in figure 4.5 (b), the lowest frequency component in the baseband spectrum and respiration induced a comparatively larger chest wall movement than heartbeat did. Figure 4.5 (c) indicates the breathing fundamental, the 2nd harmonic, and the 3rd harmonic as well as the heartbeat fundamental. Figure 4.5 (d) shows the RR and HR fundamentals only. It clearly indicates a seamless extraction of respiration signal while accurately detecting the heart rate which presents the usual main challenge for vital sign detection.

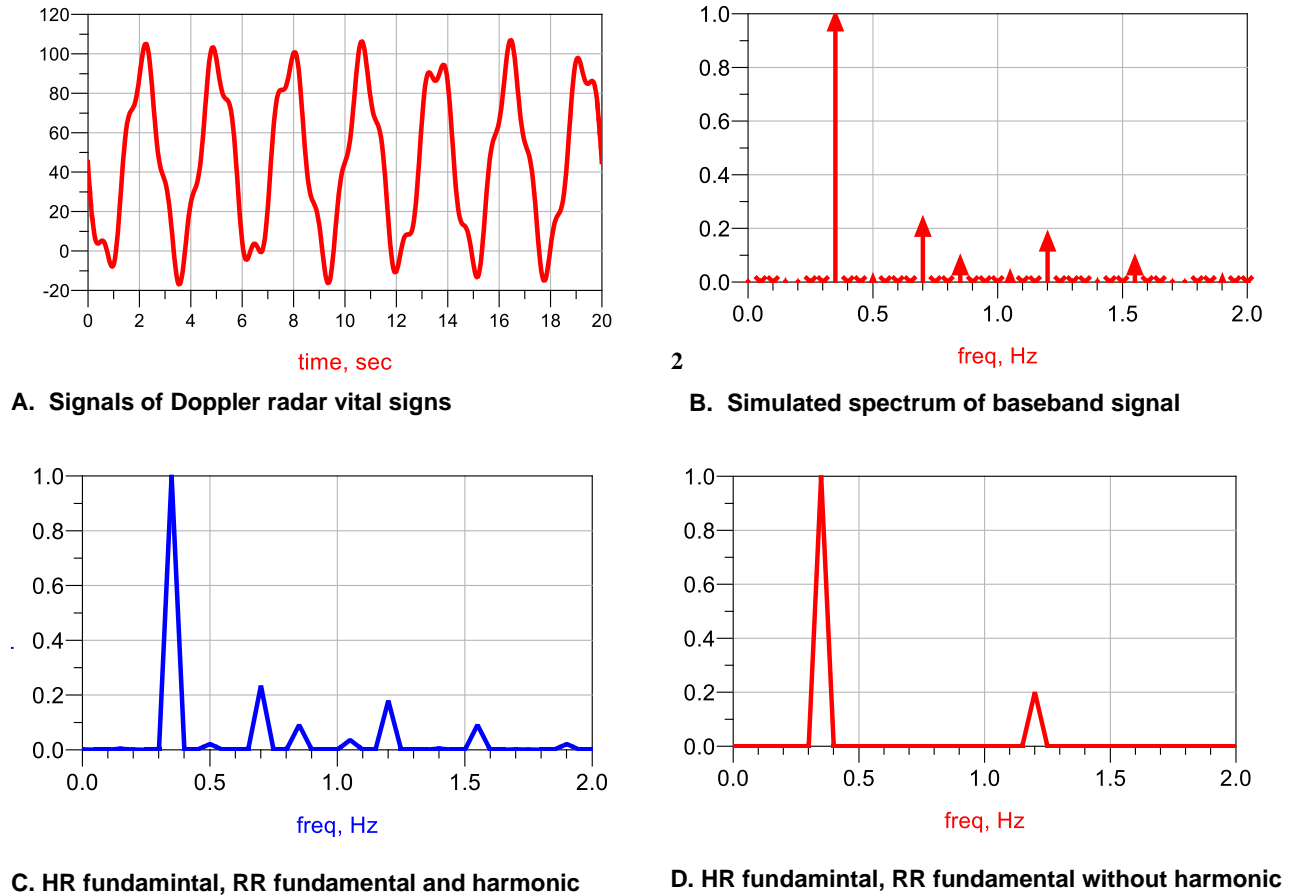


Figure 4.5 Simulated measurements of respiration rate RR, and heart rate HR performed using ADS.

### 4.3 Lab Experiment and Results

The experiment was performed at the INRS's facilities. Figure 4.8 shows an illustration of how respiration rate RR and heart rate HR are measured. It includes experiment setting and signal processing. The tracking of fine chest wall motion can be obtained by measuring the phase shift of the reflected. The acquisition of the reflected signal in the time domain. The extracted

signals contain information on respiration rate, and heart periodic movement. The algorithm employed most frequently is Fast Fourier Transform FFT and digital filtering. A band-pass filter (BPF), employed in the frequency domain, with cut-off frequencies ranges of 1.0 to 1.66 Hz and 0.2 to 0.34 Hz are used to mark heartbeat and respiration rate respectively. Heart rate and respiration rate in Hz(s) are converted to beat per minute and breath per minute.

#### 4.3.1 Experimental Procedure

Figure 4.6.a shows the block diagram of the proposed MIMO radar system setup used to measure the vital signs and bioelectrical signals (ECG, EEG) of a human target. The MIMO radar system was employed to circumvent the obstacles, such as ambiguity due to lack of range, limitations in imaging due to short observation time, and poor resistance against interferences - signal-to-noise ratio SNR, which present the usual challenges to vital signs detection. In fact, the MIMO systems deployment has dramatically improved the performance of radar systems over single antenna systems since its first use in 2003. It offers diversity gain in improving the detection/estimation performance, and spatial resolution gains in enhancing the resolution performance [108]. A Multiple-input multiple-output system also has the capability to measure the angle-of-arrival (AoA) of the received echoes thus enabling the estimation of the targets' precise location over both the azimuthal and the elevation planes [109]. A two-antenna setup MIMO system will be exploited in this study to enhance the accuracy and reliability of biosignal detection i.e., heart and brain electrical activities.

In this experiment a 7.0 GHz noncontact Doppler radar vital sign detection system is used. The components used are listed as follows: multi transmitting, receiving antennas, signal generator, mixers, oscilloscope. The carrier frequency is chosen to be 7.0 GHz, which is in the Industrial Scientific Medical band. The distance between the target and the radar is approximately 0.5 cm. The experiment was conducted on a healthy male subject, who were instructed to maintain a supine resting position and refrain from movement. The sampling rate was 1000 Hz, and measurements were collected from the subject using a digital storage oscilloscope for a duration of 7min. As shown in figure 4.6.b.

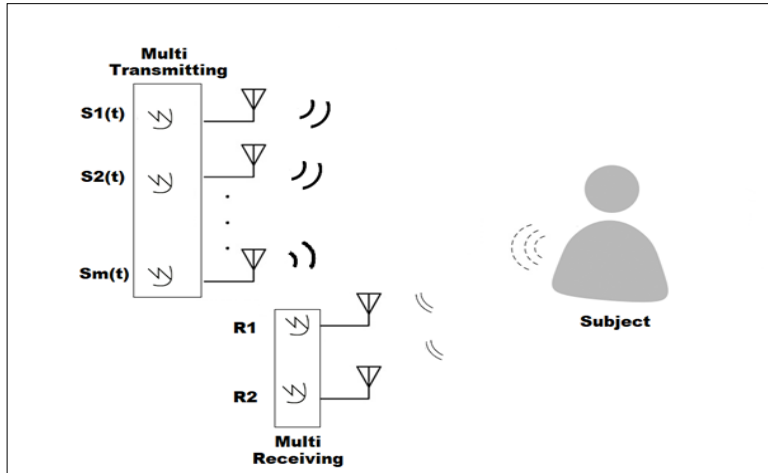


Figure 4.6. a. A block diagram illustrates the multi-input multi output setup of MiMO radar system employed to detect biosignals

The heart and respiration rate values calculated using the MatLab software, which was also used for pre-processing the signals. The computer processes wave signals to derive information suitable for viewing, e.g., by suppressing, compressing, or expanding elements or combining them with other information-bearing signals and presenting that information on a display to be plotted if so desired. MatLab software, which was also used for pre-processing the signals. Display the data after the setup as shown in figure 4.9 shown the basic steps of the preprocessing including.

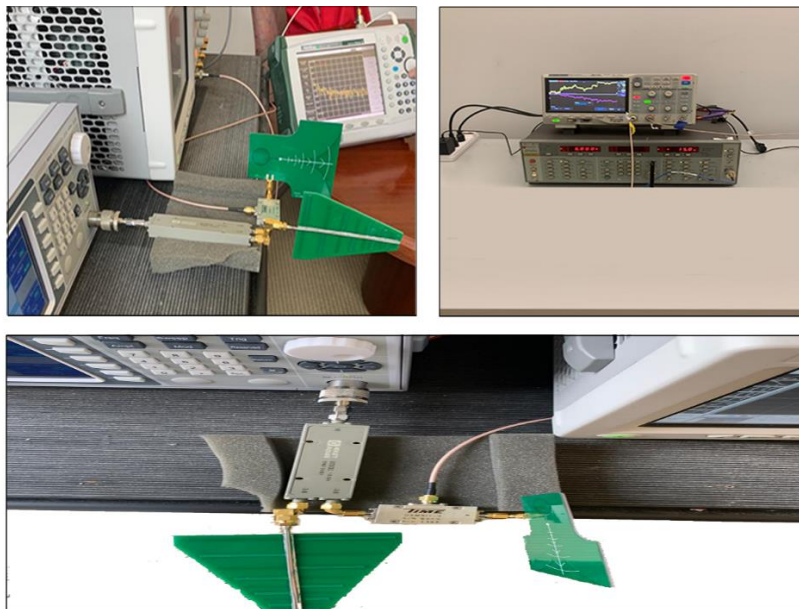
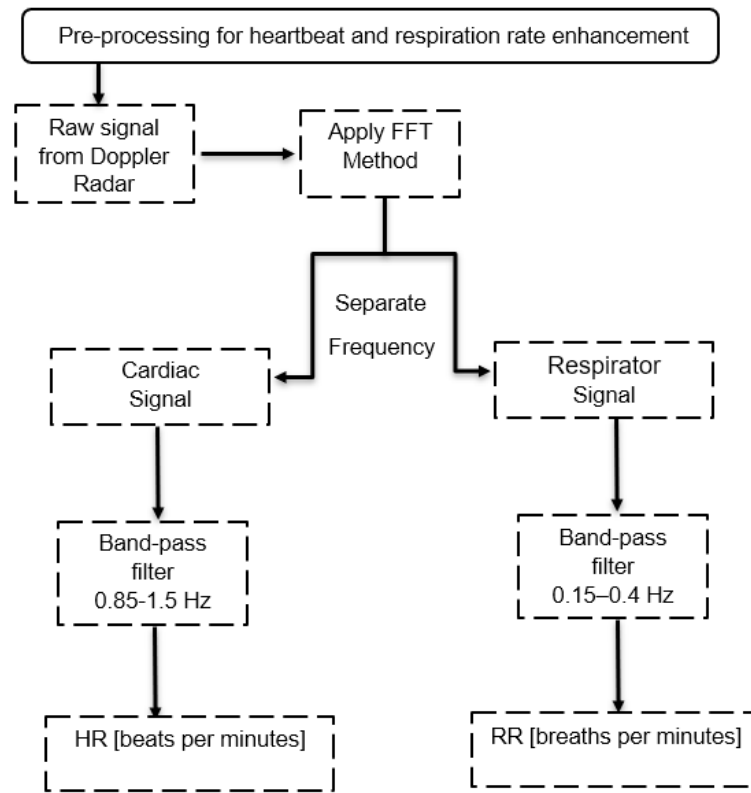


Figure 4.6.b Experimental setting for non contact biosignals measurement at INRS lab



**Figure 4.7.a shows the basic steps of the preprocessing including**

Figure 4.8 shows the raw signals of doppler radar vital signs for respiration and heartbeat. The vital signs are extracted by the radar in the time domain assuming a person is keeping still. A clutter reduction technique was applied to the raw signal to remove background noise. The time domain signals are converted into frequencies. The resulting FFT signal is plotted as shown in Figure 4.9. The extracted baseband spectrum: breathing fundamental, the 2nd and the 3rd harmonics; h1: heartbeat fundamental; c1 and c2 are the lower and upper sidebands caused by intermodulation of r1 and h1. A band-pass filter is used to recover the respiration from a mixed signal and reduce the noise as shown in figure 4.10. Figure 4.11 illustrates the result from the FFT analysis, where the peak at 0.26 Hz corresponds to the respiratory frequency (16 breaths/min). Figure 4.12 A band-pass filter is used to recover heart rate signals. Figure 4.13 illustrates the result from the FFT analysis, where the peak at 1.21 Hz corresponds to the cardiac frequency (73 beats/min). It should be noted that the heart rate in the frequency domain is easily contaminated by respiration and its harmonics, therefore it is hard to obtain an accurate heart rate.

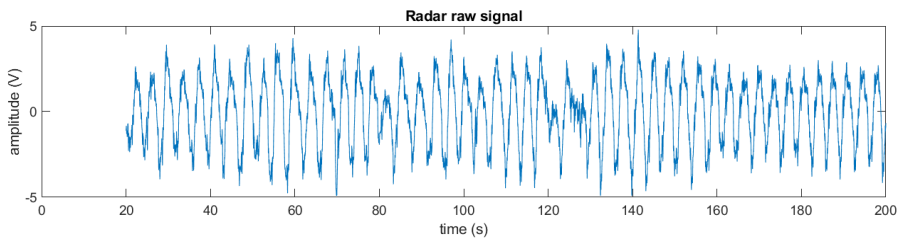


Figure 4.8 Time domain waveform of the radar result

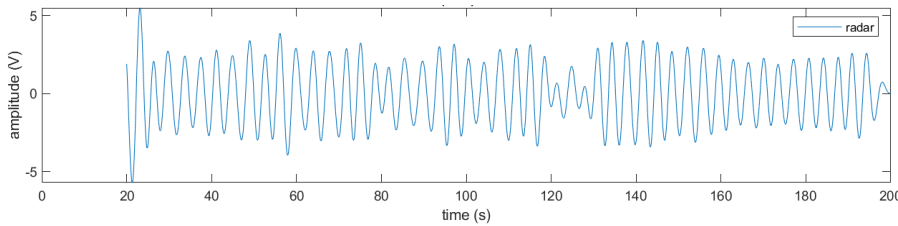


Figure 4.10. Respiratory signal

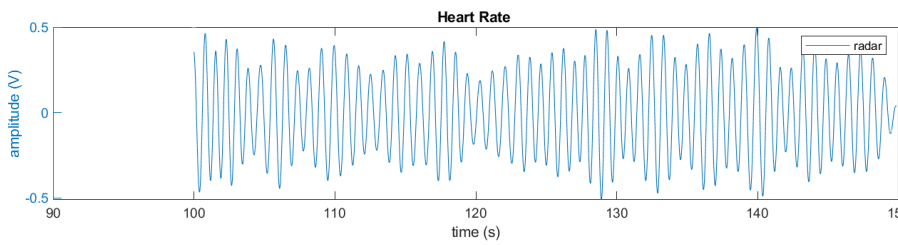


Figure 4.12. Heart rate signal

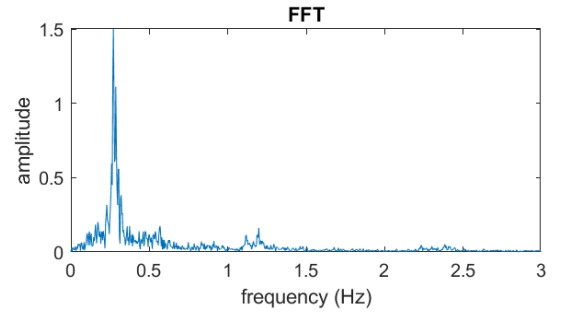


Figure 4.9 FFT signal of time domain output  
FFT RR (16 bpm)

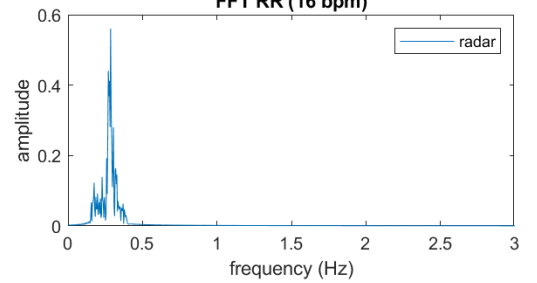


Figure 4.11 FFT of respiration signal

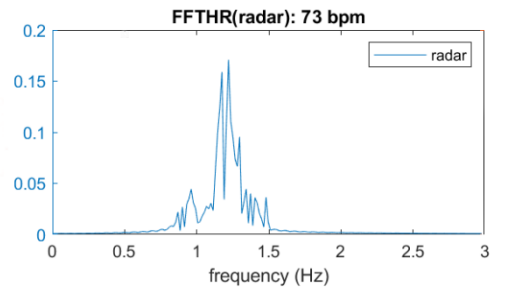


Figure 4.13. FFT of heartbeat signal



## 5 Direct Detection of Bioelectrical Signal via MIMO Radar

---

### 5.1 Biological Signal in the Human Body

A biological signal is defined as a signal that originates from a human body. Of course, such signals may exist as part of the homeostasis biological processes within an organ or be evoked by the use of an external stimulus. It is possible to group biological signals based on their physical characteristics generated naturally by stimulation. [72]. The most popular biological signals are those that are used in routine clinical practice. These are commonly as follows:

- Bioelectrical signals, which originate from the electric phenomena taking place on the membrane of cells.
- Bioacoustic signals, which entail the measurement of sounds that are generated by some organs due to fluidic or mechanical movements within the body.
- Biomechanical signals, which include measurement of the deflections in position, pace, acceleration, flow rates and pressures.
- Biochemical signals, providing information regarding the concentration of substances in the body and their pH.
- Body temperature, which reflects the metabolic interactions within the body. [72].

### 5.2 Cardio Electro-Mechanical Events

The cardiac cycle is a series of electrical and mechanical events that occur during the phases of heart relaxation (diastole) and contraction (systole). The ventricular diastolic stage involves blood flow from the atria to the ventricles, and the ventricular systole includes blood flow from the ventricles to the pulmonary artery and the aorta. Cardiac systole is the myocardial cells' mechanical response to an electrochemical stimulus originating from the sinoatrial (SA) node. By acting as a pacemaker, it controls the cardiac cycle. The electrical activity originating from the SA node propagates through the heart's fibrous skeleton (first the atrial mass, then the AV node) and the subsequent depolarization wave from top to bottom of the heart triggers the mechanical activation. The conduction of the electrical activity through the fibrous skeleton can be seen on an electrocardiogram (ECG) [4]. During each heartbeat, the ECG recording represents the electrophysiological activity and is obtained using electrodes mounted on the skin. In the same figure the conduction at the atria is shown as the P-wave and the PR interval corresponding to the delay in the AV node follows. The propagation of electrical activity across the ventricular myocardium creates the QRS complex, and the T-wave is known as ventricular

repolarization (relaxation of the muscles). In imaging devices, the ECG signal is often widely used as a gating signal to capture heart images at different phases of the heart cycle [78].

The heart undergoes repeating changes in different directions and orientations related to the cardiac cycle [79].

From the perspective of cardiac mechanical motion, the cardiac cycle represents repeating movement changes in different atrial and ventricle. Mechanical manifestation of biological system: movements, deflections, pressure, voltage, volume or flowing changes, blood pressure and expenditure of the heart. In the electrical conduction point of view, the heart transmits electrical signals generated usually by the sinoatrial node to cause contraction of the heart muscle, which in turn results in the coordinated rhythmic contraction and relaxation of the heart throughout each cardiac cycle [80]. This orderly pattern of electrical activity gives rise to the characteristic ECG measurement and tracing, which conveys a large amount of information about the structure and function of the heart.

As we mentioned already, the normal cardiac rhythm is mainly produced from the SA node, which is known as the normal pacemaker. Each depolarization is followed by repolarization in different regions of the heart, which generates currents with different magnitudes. Therefore, the combination of different activation waves from each heart region is responsible for the overall PQRST waveform. Figure 5.2 shows the normal ECG waveform as representation/characterizations of the cardiac conduction system. In general, the ECG signal contains the following waves: [81]

**P-Wave:** It is the first wave registered in the ECG, representing the atrium activation just after the sinus stimulation. It normally lasts between 60 and 90 ms in adults, has a round shape with maximal amplitude between 0.25 and 0.30 mV.

**PR-Interval:** It is measured from the start of the P-wave to the start of the QRS-Complex and lasts 90 ms.

**QRS-Complex:** It corresponds to the ventricular activation and is measured from the start of the first wave (no matter if it is Q- or R-wave), to the last wave (R- or S-wave). In normal adults, the complex lasts about 80 ms and presents a sharp shape because of the high frequencies of the signal. Its shape varies a lot, depending on the lead system used.

**ST-Interval:** It lasts from the end of the QRS-complex to the start of the T-wave and corresponds to part of the ventricular repolarization process. **T-Wave:** It represents the ventricular activation, has a round shape with amplitude about 0.60 mV. In this study we will focus on only two types of biological signal i.e., biomechanical and bioelectrical. [82]

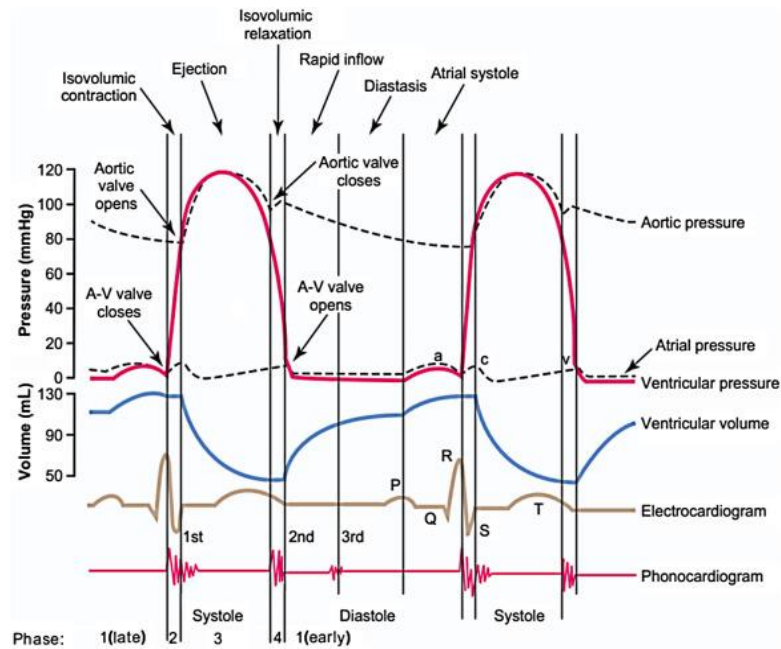


**Figure 5.2. Events of the cardiac cycle showing changes in left atrial pressure, left ventricular pressure, aortic pressure, ventricular volume, the electrocardiogram and the phonogram during systole and diastole.**

### 5.2.1 Cardiac Mechanical Signal

Cardiac muscles have a key role in the heart functions. The cardiac muscle is a kind of muscle which is found only in the heart. Cardiac muscle cells (or cardiac myocytes) are single nucleated. Ventricle myocytes have a length of about 100  $\mu\text{m}$  and a diameter of around 25  $\mu\text{m}$  (atria myocytes are smaller than ventricle myocytes) [69].

Every heartbeat creates small vibrations that shake the human body and the mechanically coupled environment around it. These vibrations can be recorded using sensors, although what all these signals have in common is the beating of the heart as their main source, these signals have different morphologies and different relationships to cardiovascular dynamics, depending on the placement and type of the sensor. The recording of the reaction movement of the centre of gravity of the body caused by the heart action has been traditionally called ballistocardiogram (BCG), whereas the local pulses include several signals with different names depending on the placement and the type of sensor used. See figure. 5.3. [61]. Cardiac induced mechanical motions are ranging from 0.2 to 0.5mm. It is also worth noticing that heart structure is often described as the size of 120mm in length, 80mm in width and 60mm in thickness approximately and the mechanical motions induced from the cardiac cycle are distributed in various parts of the precordial area around the chest [47].

### 5.2.2 Cardiac Electrical Signal

Bioelectrical signals are those that are generated by the summation of electrical potential differences across a specialized tissue or an organ. Examples of bioelectrical signals are Electrocardiogram (ECG), Electroencephalogram (EEG), Galvanic skin response (GSR), Electromyogram (EMG), Electrooculography (EOG) and Mechanomyogram (MMG). These signals are commonly used for medical diagnosis. Recent studies have shown that the bioelectrical signals can also be used as a physiological modality for human recognition [50].

A bioelectrical signal is in fact the sum of action potentials of cells at an anatomical site such as the heart, brain, or skeletal muscle. The action potential, illustrated in figure 5.2, is an electrical signal which accompanies a mechanical contraction of a single cell when stimulated by an electrical current, classified as either neural or external. This electrical signal is caused by the flow of sodium ( $\text{Na}^+$ ), potassium ( $\text{K}^+$ ), chloride ( $\text{Cl}^-$ ), and other ions across the cell membrane [47]. As shown in figure 5.3. [104].

Bioelectrical signals provide significant information regarding the nature of physiological activity at the single-cell level as well as at the organ level. Table 5.1 shows the bioelectrical signal characteristics including their anatomical origin, frequency range, amplitude range and type of measurement method. Processing methods for the bioelectrical signals are presented. [50].

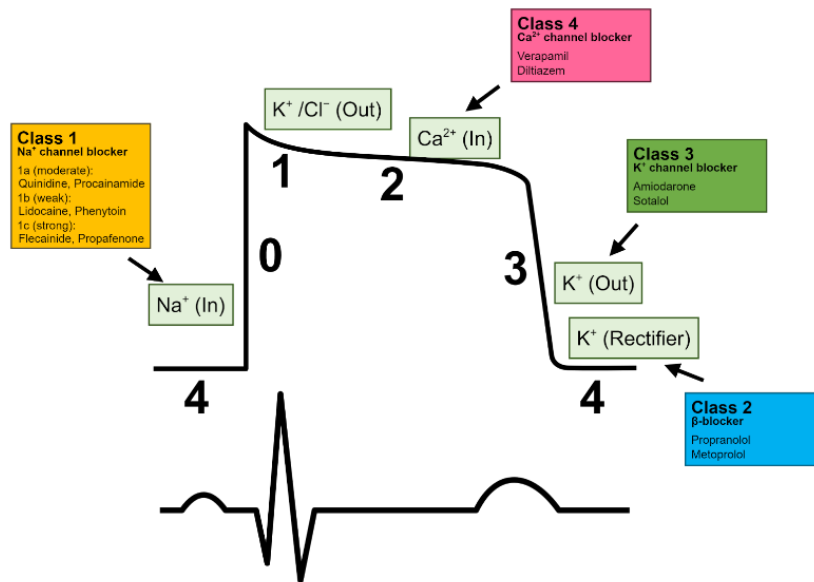
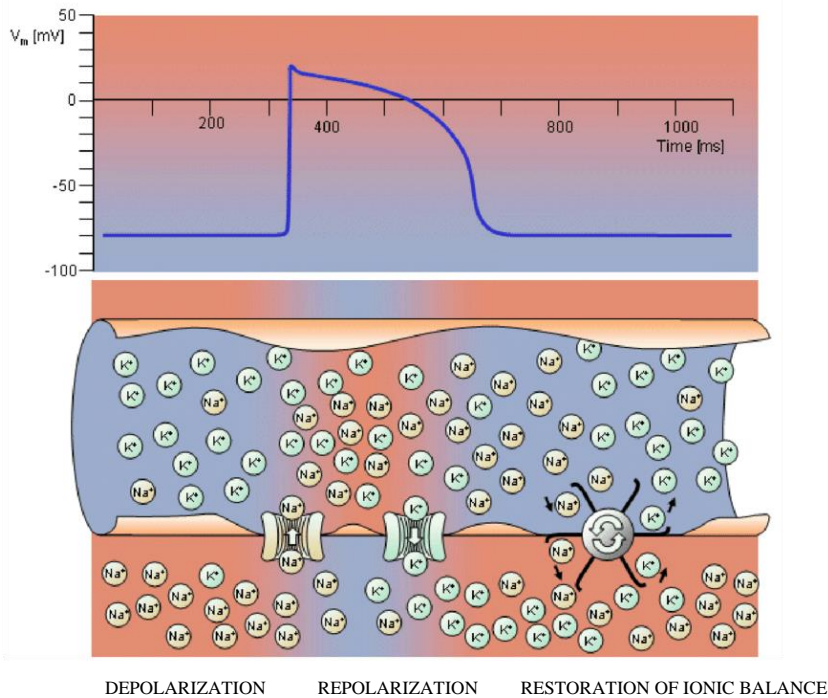


Figure 5.2. Shape of action potentials for heart



**Figure 5.3. Electrophysiology of the cardiac muscle cell**

**Table 5.1 Shown Classification of bioelectrical signals.**

Bioelectrical Signal	Signal Origin	Frequency Range (Hz)	Typical Amplitude	Measurement Method
ECG (Electrocardiogram)	Action potentials of heart muscle cells	0.05–250	0.01–5	Surface
fECG (Fetal ECG)	Fetal heart activity	0.05–250	0.01–0.02	Surface
VCG (Vectorcardiogram)	Action potentials of heart muscle cells			Surface
EEG (Electroencephalogram)	Brain neurons activity	0.1–80	0.005–0.3 0.005–10	surface intracortical
EP (Evoked Potentials)	Brain activity in reaction on external stimuli	30–3000	0.0001–0.02	Surface
ECoG (Electrocorticogram)	Signal generated by cerebral cortex	0.1–100	0.005–10	Surface
ENG (Electroneurogram)	Action potentials of peripheral nerves	0.01–1000	0.005–10	Interstitial
EMG (Electromyogram)	Action potentials of muscle fibers	0.01–10,000	0.1–10 0.05–0.3	Surface

EGG (Electrogastrogram)	Gastric muscles activity	0.02–0.15	0.01–0.5 0.1–10	surface intra gastric
EOG (Electrooculogram)	Stiff muscles activity	0.5–15	0.05–3.5	Surface
ERG (Electroretinogram)	Eye retina activity	0.2–50	0.005–1	surface
EHG (Electrohysterogram)	Uterus activity during contractions	0.1–3	0.1–5 0.1–1	surface intrauterine

Bioelectrical signals are very low amplitude and low frequency electrical signals that can be measured from biological being. Bioelectrical signals are generated from the complex self-regulatory system and can be measured through changes in electrical potential across a cell or an organ. The bioelectrical signals of our interest are in particular: the electrocardiogram (ECG) and the electroencephalogram (EEG). An ECG measures the electrical manifestation of the ionic potential of the heart while an EEG measures the electrical activity evoked along the scalp of the brain. The ECG and the EEG are recorded using standard equipment in the non-invasive fashion. The researchers of multiple disciplines have shown their greater interest in analyzing the ECG and the EEG to understand the high level features an individual is producing [96]. The analysis of bioelectrical signals therefore is widely used in assessing an individual state of health in both clinical settings and emergency sites.

### 5.3 Cardio Electrical and Mechanical Signals Correlation

The contraction of muscle is associated with electrical changes called depolarization. The electrical changes associated with contraction of the heart muscles therefore can be measured in reference to muscular contraction as shown in figure 5.4. From the perspective of cardiac mechanical motion, the cardiac cycle represents repeating movement changes in different atrial and ventricle. On the other hand, and from the electrical conduction point of view, the heart transmits electrical signals generated usually by the sinoatrial node to cause contraction of the heart muscle, which in turn results in the coordinated rhythmic contraction and relaxation of the heart throughout each cardiac cycle [40]. The contractions of the cardiac muscle cells i.e., the heart mechanical motion in this study hence can serve as a characterization of the electrical activity. This orderly pattern of electrical activity gives rise to the characteristic ECG measurement and tracing, which conveys a large amount of information about the structure and function of the heart.

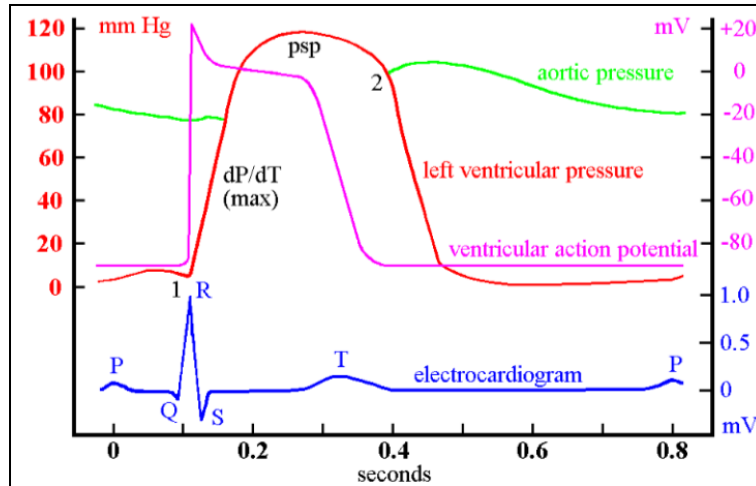


Figure 5.4. Relationship between the electrical and mechanical characteristics of the heart activity

#### 5.4 Direct Measurement of Cardiac Electrical Signal ECG

As previously stated, functioning muscles and nerves naturally generate electricity and such activity within a living body could be monitored by attaching electrodes to the body's surface. To circumvent the disadvantages of using an invasive conventional method, this work will detect and measure the heart electroactivity directly using a multi-input multi output MIMO radar system. The architecture of this type of radar, as the name suggests, has two transmitters and two receivers integrated with electric antennas. The two receiving antennas are positioned in close proximity to the chest outer surface. According to Bruce Tainio, researcher and founder of Tainio technology, the healthy body-heart is 67 to 70 MHz, the human body 62 to 78 MHz, lungs 58 to 65 MHz. [25]. The magnetic fields in the low-frequency range under consideration are extremely weak ranging from 0 to 3 kHz. and their detection requires a rather extensive laboratory equipment which rules out the use of such technique in most practical environments [5]. Therefore, an ADS is used to simulate the measurement process. Figure 5.6 presents a schematic diagram of the MIMO radar system illustrating the direct measurement of heart electrical activity via ADS.

In this section, we aim to develop a technique for conducting measurements of heart electrical activity by applying an electric field at a radio frequency (RF). The low RF power is fed to a small antenna as shown in figures 5.5. The signal is directed by the antenna to the chest of the subject being examined. The signal from the antenna penetrates the chest surface and impinges upon the tissue of the heart. Within the tissue of the heart, the signals behave, much in the manner of the conventional process techniques. The reflected wave signals are captured

using two independent electric antennas. The output signal is equal to the difference in frequencies of the two received signals. The output of the signal is subsequently fed to a computer for further processing to extract information needed for evaluation, e.g., by suppressing, compressing, or expanding elements or combining them with other information-bearing signals and presenting that information on a display to be plotted if so desired. Figure 5.7 shows a plot of the directly measured raw signal of the heart electrical activity. The resulting signal is quite comparable to that obtained using standard ECG measuring devices. The raw signal is further processed using MatLab algorithms for feature extraction i.e., P, QRS, T waves and heart rate.

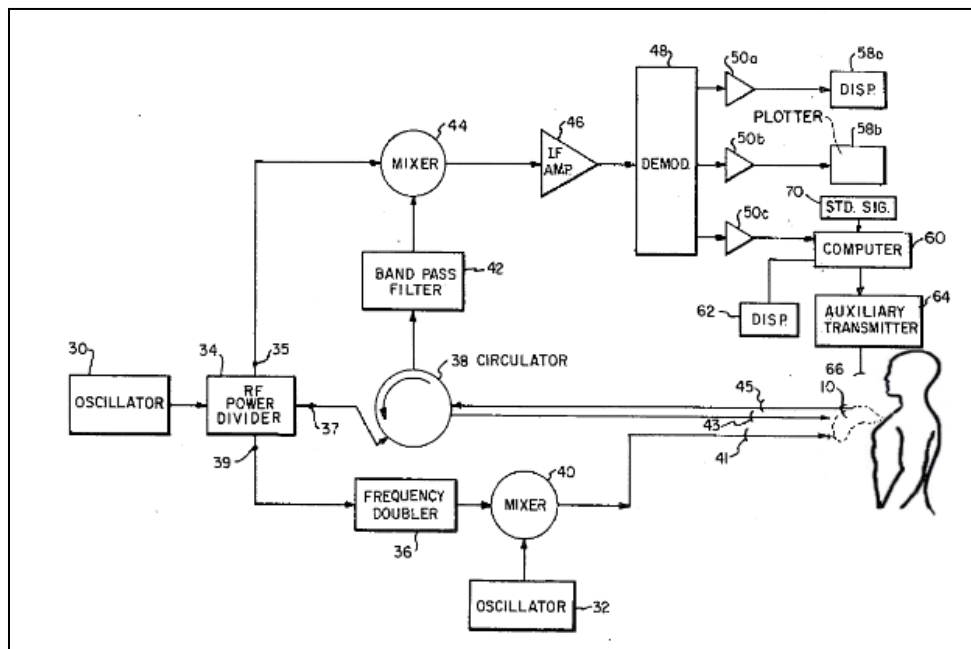


Figure 5.5 is a block diagram showing the interconnection of the components of the proposed system.

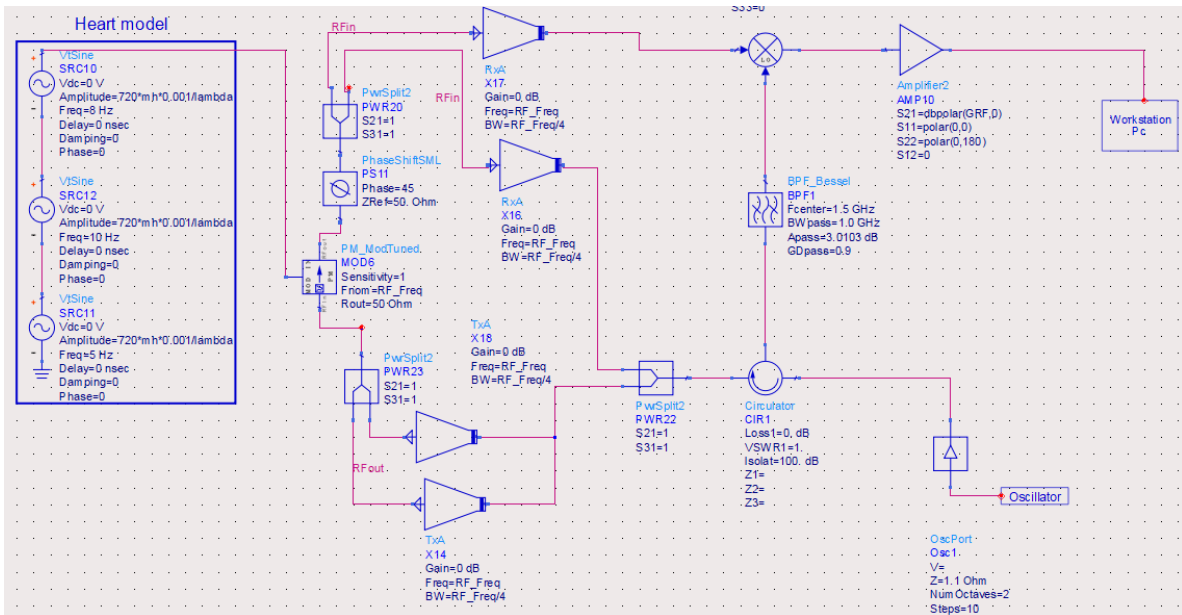


Figure 5.6 Schematic diagram of MIMO radar system illustrates the direct measurement of heart electrical activity via ADS

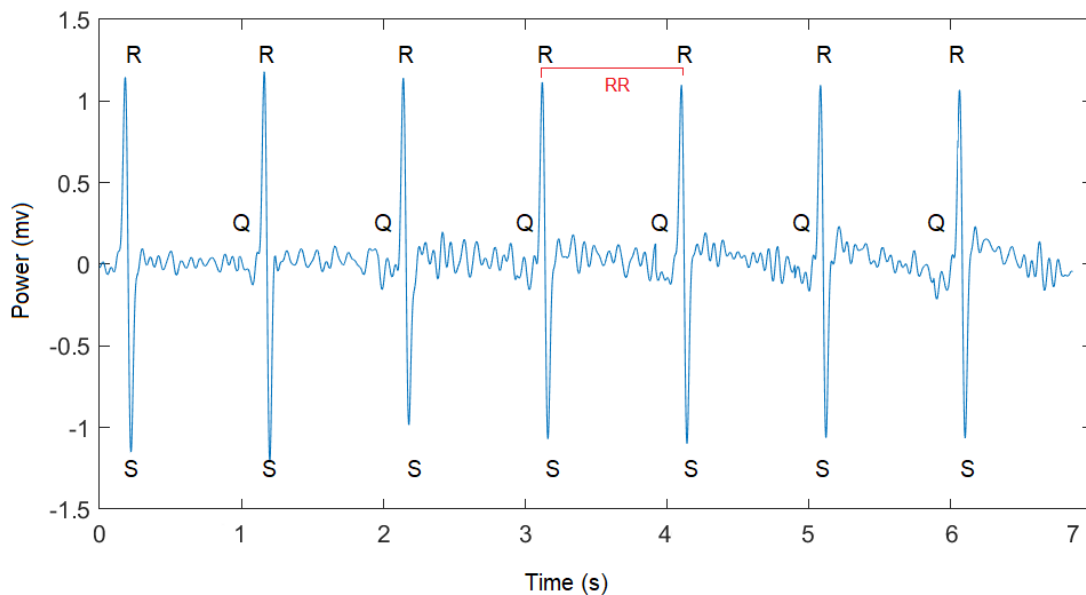


Figure 5.7 ECG signal obtained from MIMO radar system. It shows the graphical representation of the heart's electrical activity. That lead to further feature extractions. The RR interval begins at the peak of one R wave and ends at the peak of the next R wave. It represents the time between two QRS complexes. The height of the deflection also represents the amount of electrical activity flowing. The higher the deflection, the greater the amount of electrical activity. The R wave is clearly greater than the S wave. That suggests depolarisation. The QRS complex represents depolarisation of the ventricles. It closely resamples that of a normal ECG. It appears, as shown in the graph, as three closely related waves i.e. the Q, R and S waves.

## 6 Electroencephalograph Signal Detection Using MIMO Radar System

---

### 6.1 Brain Activities

The most complex “computer” in the world is the human brain. Despite numerous attempts, no one has ever managed to completely model its overall operation. It consists of as many as 100 billion neurons, and each neuron can create as many as 10,000 synaptic connections with other nerve cells. The brain is jelly-like in consistency because it is mostly water. Its mass accounts for about 2% of the total human body mass and consumes 20 % of the energy produced by the body. The very process of thinking is based on electricity and chemistry—in an active state, the brain produces energy of about 25W, which is enough to light up a light bulb. At the moment, even though, much research and extensive knowledge about the brain, there are still many unknowns. The brain is a highly homogeneous living organ, which dynamically changes over time both in structure and mechanical properties. [62]

Techniques for capturing electrical signals from the brain corresponding to most of the activities (actual or imagined) generated by neuron firing have provided neurologists with a fascinating path to decoding and studying this complex system. Technology to increase the spatiotemporal resolution of brain mapping tools has been advancing, aiming at highly dense electrode sites with the long-term stability of devices and negligible damage to brain tissue. [21]. Patients with mental disorders or individuals with ongoing signs and symptoms of mental illness need constant monitoring of their conditions. Thus, the need for non-invasive diagnosis systems or devices such as electroencephalography EEG exams is crucial [80]. Structure of a typical neuron as shown in figure 6.1 The delay in detecting or diagnosis of mental health disorder or symptoms is detrimental.

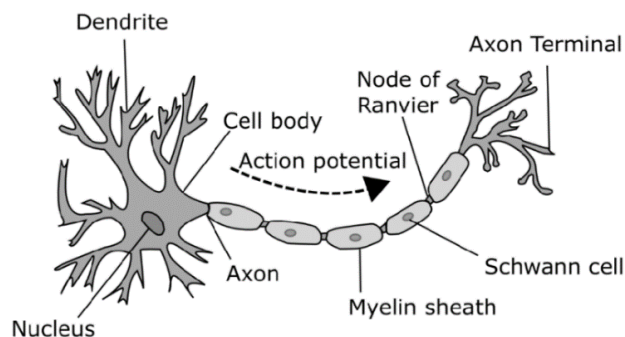


**Figure 6.1. Biological Structure of a Typical Neuron**

## 6.2 Electroencephalography

Electroencephalography (EEG), a tool proved to be a crucial tool in brain research and monitoring brain activity, is usually applied for the purpose of neurological and psychological disorders or epileptic seizures examination. It is also used for monitoring various stages of sleep. Another implementation of electroencephalography is brain interaction with external environments in the form of Brain-Computer Interface (BCI) systems. EEG is a diagnostic method, enabling measurement and recording of the electrical activity of the brain. The measurement of the EEG can be classified as either invasive or non-invasive, depending on surgical intervention necessity. The non-invasive measurement method is based on electrodes placed on the scalp, in accordance with the “10–20” system, as illustrated in figure 6.2. The invasive recordings require e.g., needle electrodes [26].

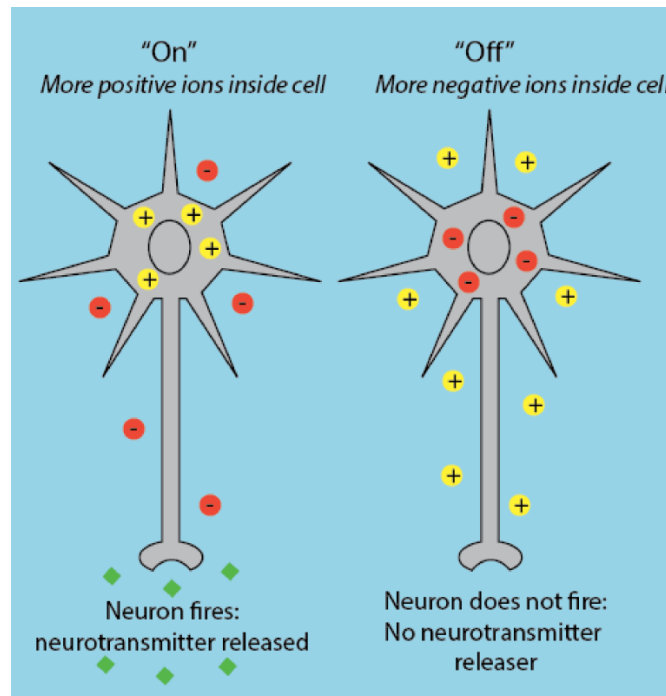


Figure 6.2 Understanding neuronal activity

In general, more positive ions inside the cell relative to the outside result in the neuron firing and thus releasing neurotransmitters. When more negative ions are inside the cell relative to the outside, the neuron does not fire, so no neurotransmitter is released. Positive ions are represented as yellow circles with '+' sign, negative ions are represented as yellow circles with '-' sign, green diamonds represent neurotransmitters.

EEG waves - indicative of the brain state - are recorded using the electrodes within the below listed ranges, which correspond with the individual frequency domains as illustrated in figure 6.3 [7].

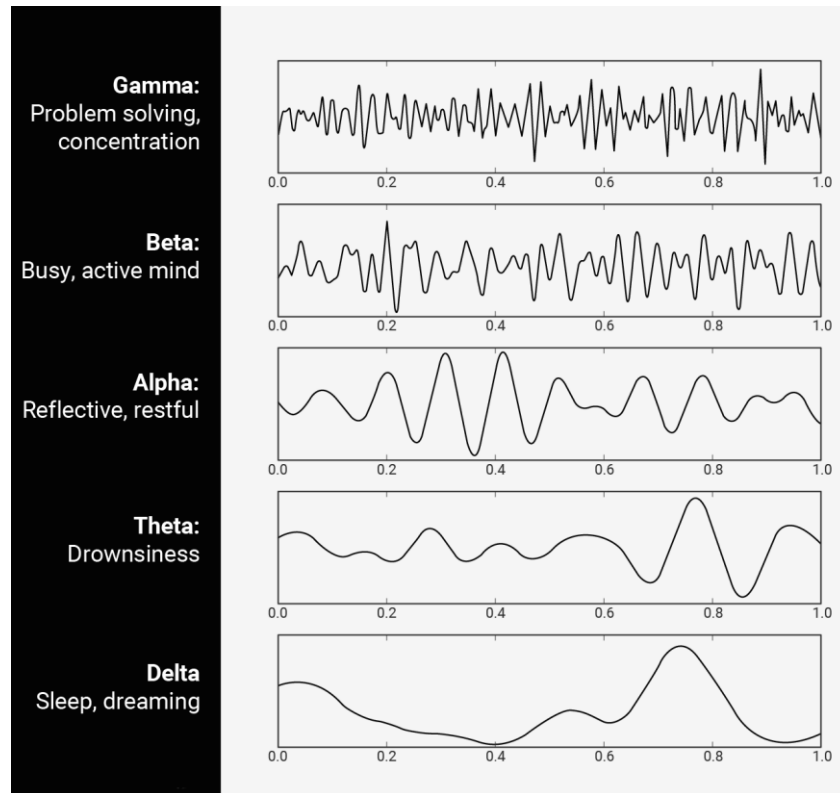
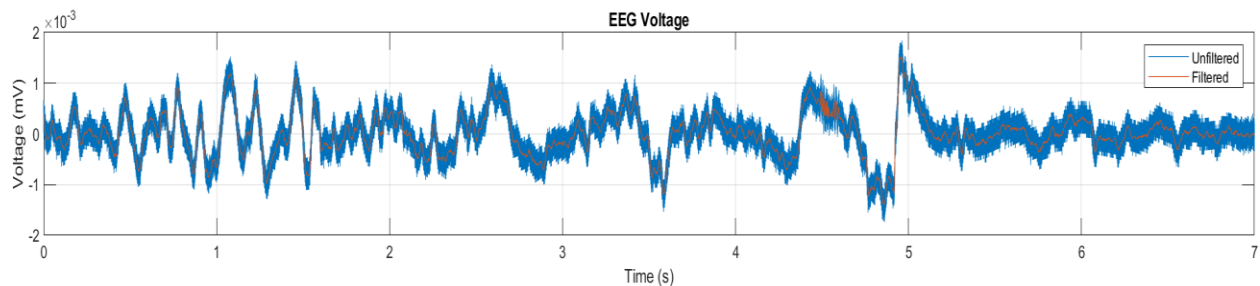


Figure.6.4 Illustration of different types of brain waves that are reflective of brain state

### 6.3 EEG Monitoring Using Contactless MIMO Radar System

According to Bruce Tainio, researcher and founder of Tainio technology, the healthy body brain frequency ranges 72 to 90 MHz, and normal brain frequency 72 MHz [99]. Functioning muscles and nerves naturally generate electricity. Such activity, within a living body, is monitored conventionally by attaching electrodes to the scalp. To overcome the disadvantages of using invasive conventional methods. This work intends to directly detect and measure the brain electroactivity using RF waves MIMO radar system. The magnetic fields in the low frequency range under consideration are extremely weak and their detection requires rather extensive laboratory equipment which precludes the use of this technique in most practical environments. This work aims to develop a technique for conducting measurements of the brain activity by applying an electric field at a radio frequency. Low RF power is fed to an electro antenna as shown in figure 6.5. The signal is directed by the antenna to the scalp of the subject being

examined. The signal from the antenna penetrates the scalp bone and impinges upon the cells of the brain. Within the cells of the brain, the signals behave, much in the manner of a conventional wave propagation. The reflected wave signals are captured using two independent electric antennas. A charges separation circuit is employed to split the positive and the negative charges. DC charge controller is used to ensure sufficient and stable electricity is fed to an EEG circuit. The output of the EEG circuit is subsequently fed to a microcontroller. The computer processes the output signals to obtain information needed for further features extraction. The results obtained in the INRS laboratory are then presented on a display and plotted as shown in figure 6.6.



**Figure 6.5** A plot of detected EEG signal before and after applying Band pass filter.

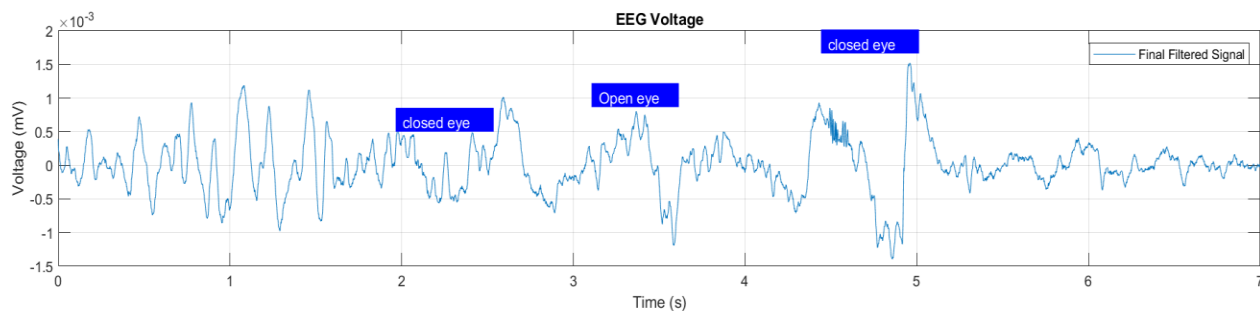


**Figure 6.6** A plot of results of the EEG signal obtained from the MIMO radar system on a time (in seconds) versus voltage (in mv) graph. It shows that the signal with the brain cells behaves much in the manner of conventional wave propagation. The EEG signal is a manifestation of the brain activity of a healthy human subject- crosspans to Beta wave exhibited in figure 6.4 (busy, active mind). To the left of graph, the subject's eyes were closed and to the right of the graph the subject's eyes were wide open. The steady to low fluctuation i.e. when eyes were closed and high fluctuation when eyes were wide open. The degree of the fluctuation is indicative of the level of brain activity or state of mind.

## 7 CONCLUSION

---

We have demonstrated a novel doppler radar based biosignal monitoring system that offers a non-invasive continuous monitoring of respiratory and heart rates as well as bioelectrical activity i.e., ECG and EEG signals for the first time. The concept is based on Multiple Doppler radar system with one or more frequency. Several experimental and simulation techniques were employed to overcome challenges such as ambiguity due to lack of range, limitations in imaging due to short observation time, and poor resistance against interferences - signal-to-noise ratio SNR.

Since the cause of the radar detected signal could correlate to heartbeat, breath, or blood perfusing, we proposed a method to study and quantify electromagnetic radiation and human body interaction. Ansys HFSS was employed to examine the said interaction, to consolidate our knowledge and to answer the question of what is actually measured in a noncontact doppler radar vital signs detection. Based on swept-frequency techniques, several runs at incremental frequencies of 0.5, 1, 5.7, 20 and 70 GHz were performed. The simulation software was also used to accurately measure the frequency dependent parameters during the scattering of the EM waves on the target's different tissues' interface i.e., skin, muscles, bones, fat, lungs, and heart.

Guided by the results obtained from the measurement of the EM waves and human tissues interaction, lab experiments, simulation softwares and algorithms were employed to measure the respiration rate RR and heart rate HR. Furthermore, in this thesis we used standard breathing rate heartbeat listed in reputable medical authorities' references such as the American Heart Association to avoid significant discrepancies and limitations present in previous works.

Even though detecting heart rate presents a usual main challenge for vital sign detection because respiration induces a comparatively larger chest wall movement than heartbeat did, a seamless extraction of respiration signal while accurately measuring the heart rate. The experiment measurement values obtained were: heart rate is 72 bpm, and respiration is 16 bpm. To further illustrate the effect of respiration interference on the detection of heart rate, we performed a second experiment from the backside. The amplitude of the detected heartbeat signal from the backside was much higher than when measured from the front side. That clearly indicates less interference from respiration fundamentals and its harmonics on heartbeat signals.

We further exploited the possibility of directly sensing bioelectrical cardiac and brain activity. The multi-input multi output MIMO radar system leverages the two transmitters and two receivers integrated with electric antennas. ADS was used to simulate the MIMO measurement process. Since the magnetic fields in the low-frequency range under consideration were extremely weak - ranging from 0 to 3 kHz, and their detection requires a rather extensive laboratory equipment. The initial results obtained however prove promising further direct sensing system development.

Finally, we provided evidence of the feasibility and potential of the MIMO radar as a contactless biosignals monitoring system through extensive experiments. Our evaluation in this thesis has focused on integrating both actual EM wave tissues interaction measurements and advanced processing techniques. It would be very interesting, as the research evolves, to evaluate the system's performance in medical applications. And its contribution in terms of cost reduction, efficiency and better patients' experience.

## **7.1 Recommendation and Future work**

This research designed and developed a novel patient-centered non invasive radar techniques to provide vital sign detection needed in health centres, homes for disastrous areas. To further develop the work done, we propose to undertake the following project ideas in the future:

- Even though the results obtained using the MIMO radar system were promising and satisfactory, there is still room for further future development of this system. Furthermore, we intend to exploit the addition and integration of suitable / adequate electrical antennas.
- We have explored an array of signal processing techniques to overcome the challenges of extraneous noises and limitations due to short observation time. Therefore, we highly recommend the implementation of even faster and more accurate techniques such as quantum sensing.
- Further study and experiments need to better detect signals due to blood transfusion to measure blood pressure using MIMO FMCW doppler radar. Work could also be extended to measure other vital signs such as body temperature.



## REFERENCES

---

- [1] Kashou AH, Basit H, Chhabra L. Physiology, Sinoatrial Node. [Updated 2021 Oct 9]. In: StatPearls [Internet]. Treasure Island (FL): StatPearls Publishing; 2022 Jan-. Available from: <https://www.ncbi.nlm.nih.gov/books/NBK459238>
- [2] Anitori, L., de Jong, A., & Nennie, F. (2009). FMCW radar for life-sign detection. IEEE National Radar Conference - Proceedings. <https://doi.org/10.1109/RADAR.2009.4976934>
- [3] Lee, J. Y., & Lin, J. C. (1985). A Microprocessor-Based Noninvasive Arterial Pulse Wave Analyzer. IEEE Transactions on Biomedical Engineering, BME-32(6), 451–455. <https://doi.org/10.1109/TBME.1985.325454>
- [4] Lakshmi, I. (2021). Anatomical photo representations for cardiac imaging training. In Image Processing for Automated Diagnosis of Cardiac Diseases (pp. 35–48). Elsevier. <https://doi.org/10.1016/B978-0-323-85064-3.00005-4>
- [5] APPARATUS AND METHOD FOR REMOTELY MONITORING AND ALTERING BRAN WAVES Inventor, Robert G. Malech, Plainview, N.Y. Assignee: Dorne and Margolin Inc., Bohemia, N.Y. Filed: Aug. 5, 1974
- [6] Iyer, S., Zhao, L., Mohan, M. P., Jimeno, J., Siyal, M. Y., Alphones, A., & Karim, M. F. (2022). mm-Wave Radar-Based Vital Signs Monitoring and Arrhythmia Detection Using Machine Learning. Sensors, 22(9). <https://doi.org/10.3390/s22093106>
- [7] <https://www.bitbrain.com/blog/alpha-brain-waves>
- [8] Quiroz-Juarez, M. A., Jimenez-Ramirez, O., Vazquez-Medina, R., Ryzhii, E., Ryzhii, M., & Aragon, J. L. (2018). Cardiac Conduction Model for Generating 12 Lead ECG Signals with Realistic Heart Rate Dynamics. IEEE Transactions on Nanobioscience, 17(4), 525–532. <https://doi.org/10.1109/TNB.2018.2870331>
- [9] Chioukh, L., Boutayeb, H., Deslandes, D., & Wu, K. (2014). Noise and sensitivity of harmonic radar architecture for remote sensing and detection of vital signs. IEEE Transactions on Microwave Theory and Techniques, 62(9), 1847–1855. <https://doi.org/10.1109/TMTT.2014.2343934>
- [10] Luz, E. J. da S., Schwartz, W. R., Cámara-Chávez, G., & Menotti, D. (2016). ECG-based heartbeat classification for arrhythmia detection: A survey. Computer Methods and Programs in Biomedicine, 127, 144–164. <https://doi.org/10.1016/j.cmpb.2015.12.008>
- [11] Sattar Y, Chhabra L. Electrocardiogram. [Updated 2021 Jul 31]. In: StatPearls [Internet]. Treasure Island (FL): StatPearls Publishing; 2022 Jan-. Available from: <https://www.ncbi.nlm.nih.gov/books/NBK549803/>
- [12] Muñoz-Ferreras, J.-M., Wang, J., Peng, Z., Gómez-García, R., & Li, C. (n.d.). From Doppler to FMCW Radars for Non-Contact Vital-Sign Monitoring.
- [13] Connor, G., & Melia, R. (2013). Electromagnetic Absorption by the Human Body from 1 to 15 GHz.
- [14] S. Gabriel, R. Lau, and C. Gabriel, “The dielectric properties of biological tissues—III: Parametric models for the dielectric spectrum of tissues,” Phys. Med. Biol., vol. 41, pp. 2271–2293, Nov. 1996.
- [15] Rothschild, J. M., Esteban Gandara, P., Seth Woolf, P., Williams, D. H., & Bates, D. W. (2010). Single-Parameter Early Warning Criteria to Predict Life-Threatening Adverse

Events.

- [16] Kebe, M., Gadhafi, R., Mohammad, B., Sanduleanu, M., Saleh, H., & Al-qutayri, M. (2020). Human vital signs detection methods and potential using radars: A review. In *Sensors (Switzerland)* (Vol. 20, Issue 5). MDPI AG. <https://doi.org/10.3390/s20051454>
- [17] Chaudhry R, Miao JH, Rehman A. *Physiology, Cardiovascular*. [Updated 2021 Nov 14]. In: StatPearls [Internet]. Treasure Island (FL): StatPearls Publishing; 2022 Jan-. Available from: <https://www.ncbi.nlm.nih.gov/books/NBK493197/>
- [18] Shafiq, G., & Veluvolu, K. C. (2014). Surface chest motion decomposition for cardiovascular monitoring. *Scientific Reports*, 4. <https://doi.org/10.1038/srep05093>
- [19] Bui, N. T., & Byun, G. S. (2021). The comparison features of ecg signal with different sampling frequencies and filter methods for real-time measurement. *Symmetry*, 13(8). <https://doi.org/10.3390/sym13081461>
- [20] Chioukh, L., Boutayeb, H., Li, N., Yahia, L., & Wu, K. (2009). Integrated radar systems for precision monitoring of heartbeat and respiratory status. *APMC 2009 - Asia Pacific Microwave Conference 2009*, 405–408. <https://doi.org/10.1109/APMC.2009.5384514>
- [21] Thukral, A., Ershad, F., Enan, N., Rao, Z., & Yu, C. (2018). Soft Ultrathin Silicon Electronics for Soft Neural Interfaces: A Review of Recent Advances of Soft Neural Interfaces Based on Ultrathin Silicon. In *IEEE Nanotechnology Magazine* (Vol. 12, Issue 1, pp. 21–34). Institute of Electrical and Electronics Engineers Inc. <https://doi.org/10.1109/MNANO.2017.2781290>
- [22] Thi Phuoc Van N, Tang L, Demir V, Hasan SF, Duc Minh N, Mukhopadhyay S. Review- Microwave Radar Sensing Systems for Search and Rescue Purposes. *Sensors (Basel)*. 2019 Jun 28;19(13):2879. doi: 10.3390/s19132879. PMID: 31261726; PMCID: PMC6650952.
- [23] [https://commons.wikimedia.org/wiki/File:2018\\_Conduction\\_System\\_of\\_Heart.jpg](https://commons.wikimedia.org/wiki/File:2018_Conduction_System_of_Heart.jpg)
- [24] Kim JY, Dao H. *Physiology, Integument*. [Updated 2022 May 8]. In: StatPearls [Internet]. Treasure Island (FL): StatPearls Publishing; 2022 Jan-. Available from: <https://www.ncbi.nlm.nih.gov/books/NBK554386/>
- [25] Hamlaoui, K. (n.d.). The human body frequency. <https://www.researchgate.net/publication/340232697>
- [26] Byrom B, McCarthy M, Schueler P, Muehlhausen W. Brain Monitoring Devices in Neuroscience Clinical Research: The Potential of Remote Monitoring Using Sensors, Wearables, and Mobile Devices. *Clin Pharmacol Ther*. 2018 Jul;104(1):59-71. doi: 10.1002/cpt.1077. Epub 2018 Apr 18. PMID: 29574776; PMCID: PMC6032823.
- [27] Cheng, J. H., Yeh, J. F., Yang, H. Y., Tsai, J. H., Lin, J., & Huang, T. W. (2012). 40-GHz vital sign detection of heartbeat using synchronized motion technique for respiration signal suppression. *European Microwave Week 2012: "Space for Microwaves"*, EuMW 2012, Conference Proceedings - 42nd European Microwave Conference, EuMC 2012, 21–24. <https://doi.org/10.23919/eumc.2012.6459289>
- [28] Lee, Y. S., Pathirana, P. N., Steinfort, C. L., & Caelli, T. (2014). Monitoring and Analysis of Respiratory Patterns Using Microwave Doppler Radar. *IEEE Journal of Translational Engineering in Health and Medicine*, 2. <https://doi.org/10.1109/JTEHM.2014.2365776>
- [29] J. -H. Lee and S. -O. Park, "A 14 GHz non-contact radar system for long range heart rate detection," 2013 Proceedings of the International Symposium on Antennas & Propagation, 2013, pp. 204-206.

- [30] Physiology, Respiratory Rate Book
- [31] Hsu, T.-W., & Tseng, C.-H. (2016). Compact 24-GHz Doppler Radar Module for Non-Contact Human Vital-Sign Detection.
- [32] Hamilton, H., Beard, J. D., Carmean, R. E., & Kory, R. C. (1985). Electrode guarding in electrical impedance measurement of physiological systems-A critique. In IEEE TRANSACTIONS ON BIOMEDICAL ENGINEERING (Vol. 15, Issue 6).
- [32] Moll, J., K. Bechtel, B. Hils, and V. Krozer, "Mechanical Vibration Sensing for Structural Health Monitoring Using a Millimeter-Wave Doppler Radar Sensor," in 7th European Workshop on Structural Health Monitoring (EWSHM), Nantes, France, 2014, pp. 1802–1808.
- [33] Chioukh, L., Boutayeb, H., Li, N., Yahia, L., & Wu, K. (2009). Integrated radar systems for precision monitoring of heartbeat and respiratory status. APMC 2009 - Asia Pacific Microwave Conference 2009, 405–408. <https://doi.org/10.1109/APMC.2009.5384514>
- [34] Van, N. T. P., Tang, L., Demir, V., Hasan, S. F., Minh, N. D., & Mukhopadhyay, S. (2019). Review-microwave radar sensing systems for search and rescue purposes. *Sensors (Switzerland)*, 19(13). <https://doi.org/10.3390/s19132879>
- [35] Chourpiliadis, C., & Bhardwaj, A. (2021). Physiology, Respiratory Rate. <https://www.ncbi.nlm.nih.gov/books/NBK537306/>
- [36] National Institute of Standards and Technology Technical Note Natl. Inst. Stand. Technol., Tech. Note 1554. 32 pages (July 2010) CODENNTNOEF
- [37] United States Patent. Sharpe et al, NON-CONTACT WITAL SIGNS MONITOR  
Inventors: Steven M. Sharpe, Atlanta; Joseph Seals, Stone Mountain; Anita H. Ga.  
Appl. No.: 213,783 Filed: Jun. 30, 1988
- [38] De Goederen, R., Pu, S., Silos Viu, M., Doan, D., Overeem, S., Serdijn, W. A., Joosten, K. F. M., Long, X., & Dudink, J. (2021). Radar-based sleep stage classification in children undergoing polysomnography: a pilot-study. *Sleep Medicine*, 82, 1–8. <https://doi.org/10.1016/j.sleep.2021.03.022>
- [39] Yen, H. T., Kurosawa, M., Kirimoto, T., Hakozaki, Y., Matsui, T., & Sun, G. (2022). A medical radar system for non-contact vital sign monitoring and clinical performance evaluation in hospitalized older patients. *Biomedical Signal Processing and Control*, 75. <https://doi.org/10.1016/j.bspc.2022.103597>
- [40] Pathirana P. N., Herath S. C. K., and Savkin A. V., "Multitarget tracking via space transformations using a single frequency continuous wave radar," *IEEE Trans. Signal Process.*, vol. 60, no. 10, pp. 5217–5229, Oct. 2012.
- [41] S. Guan, J. A. Rice, C. Li, and C. Gu, "Automated DC Offset Calibration Strategy for Structural Health Monitoring Based on Portable CW Radar Sensor," *IEEE Transactions on Instrumentation and Measurement*, vol. 63, no. 12, pp. 3111–3118, Dec. 2014.
- [42] Lakshmi, I. (2021). Anatomical photo representations for cardiac imaging training. In *Image Processing for Automated Diagnosis of Cardiac Diseases* (pp. 35–48). Elsevier. <https://doi.org/10.1016/B978-0-323-85064-3.00005-4>
- [43] Muñoz-Ferreras, J.-M., Wang, J., Peng, Z., Gómez-García, R., & Li, C. (n.d.). From Doppler to FMCW Radars for Non-Contact Vital-Sign Monitoring.
- [44] Wang, Y., Wang, W., Zhou, M., Ren, A., & Tian, Z. (2020). Remote monitoring of human vital signs based on 77-GHZ MM-WAVE FMCW radar. *Sensors (Switzerland)*, 20(10). <https://doi.org/10.3390/s20102999>
- [45] Park, J. H., Jeong, Y. J., Lee, G. E., Oh, J. T., & Yang, J. R. (2019). 915-MHz

- continuous-wave doppler radar sensor for detection of vital signs. *Electronics* (Switzerland), 8(5). <https://doi.org/10.3390/electronics8050561>
- [46] Pierdomenico, S. D., Bucci, A., Lapenna, D., Cuccurullo, F., & Mezzetti, A. (2001). Clinic and ambulatory heart rate in sustained and white-coat hypertension. In *Blood Pressure Monitoring* (Vol. 6). Lippincott Williams & Wilkins.
- [47] Chen, J., Zhang, D., Wu, Z., Zhou, F., Sun, Q., & Chen, Y. (2021). Contactless Electrocardiogram Monitoring with Millimeter Wave Radar. <http://arxiv.org/abs/2112.06639>
- [48] <https://medlineplus.gov/ency/images/ency/fullsize/1135.jpg>
- [49] Transmission of Electromagnetic Power Through a Biological Medium. B.Tech., Indian Institute of Technology. Ripan Das.2003
- [50] Connor, G., & Melia, R. (2013). Electromagnetic Absorption by the Human Body from 1 to 15 GHz.
- [51] Ostadfar, A. (2016). Biofluid Dynamics in Human Organs. In *Biofluid Mechanics* (pp. 111–204). Elsevier. <https://doi.org/10.1016/b978-0-12-802408-9.00004-1>
- [52] Al-Mallah, M. H., Juraschek, S. P., Whelton, S., Dardari, Z. A., Ehrman, J. K., Michos, E. D., Blumenthal, R. S., Nasir, K., Qureshi, W. T., Brawner, C. A., Keteyian, S. J., & Blaha, M. J. (2016). Sex Differences in Cardiorespiratory Fitness and All-Cause Mortality: The Henry Ford Exercise Testing (FIT) Project. *Mayo Clinic Proceedings*, 91(6), 755–762. <https://doi.org/10.1016/j.mayocp.2016.04.002>
- [53] Pan, K. (2021). Vital Signs Monitoring Based On UWB Radar.
- [54] Zhang, T., Sarrazin, J., Valerio, G., & Istrate, D. (2018). Estimation of human body vital signs based on 60 ghz doppler radar using a bound-constrained optimization algorithm. *Sensors* (Switzerland), 18(7). <https://doi.org/10.3390/s18072254>
- [55] Parker, M. (2017). Radar Basics. In *Digital Signal Processing 101* (pp. 231–240). Elsevier. <https://doi.org/10.1016/b978-0-12-811453-7.00018-4>
- [56] Aardal, Ø., & Hammerstad, J. (2010). Medical radar literature overview.
- [57] Kuutti, J., Paukkunen, M., Aalto, M., Eskelinen, P., & Sepponen, R. E. (2015). Evaluation of a Doppler radar sensor system for vital signs detection and activity monitoring in a radio-frequency shielded room. *Measurement: Journal of the International Measurement Confederation*, 68, 135–142. <https://doi.org/10.1016/j.measurement.2015.02.048>
- [58] Muñoz-Ferreras, J.-M., Wang, J., Peng, Z., Gómez-García, R., & Li, C. (n.d.). From Doppler to FMCW Radars for Non-Contact Vital-Sign Monitoring.
- [59] Amin, M.G. (Ed.). (2017). *Radar for Indoor Monitoring: Detection, Classification, and Assessment* (1st ed.). CRC Press. <https://doi.org/10.1201/9781315155340>
- [60] R. Srinivasan, P.L. Nunez, *Electroencephalography*, Editor(s): V.S. Ramachandran, *Encyclopedia of Human Behavior* (Second Edition), Academic Press, 2012, Pages 15-23, ISBN 9780080961804, <https://doi.org/10.1016/B978-0-12-375000-6.00395-5>.
- [61] Golemati, S., & Nikita, K. S. (n.d.). *Series in Bioengineering Cardiovascular Computing-Methodologies and Clinical Applications*. <http://www.springer.com/series/10358>
- [62] Budday, S., & Kuhl, E. (2020). Modeling the life cycle of the human brain. In *Current Opinion in Biomedical Engineering* (Vol. 15, pp. 16–25). Elsevier B.V. <https://doi.org/10.1016/j.cobme.2019.12.009>

- [63] T. Jaeschke, C. Bredendiek, S. Kuppers, and N. Pohl, "High-Precision D-Band FMCW Radar Sensor Based on a Wideband SiGe-Transceiver MMIC," *IEEE Transactions on Microwave Theory and Techniques*, vol. 62, no. 12, pp. 3582–3597, Dec. 2014.
- [64] Vital Signs Monitoring Based On UWB Rada. Master of Applied Science at Concordia University. Keyu Pan, 2021.
- [65] Korshøj, M., Lidegaard, M., Kittel, F., van Herck, K., de Backer, G., de Bacquer, D., Holtermann, A., & Clays, E. (2015). The relation of ambulatory heart rate with all-cause mortality among middle-aged men: A Prospective Cohort Study. *PLoS ONE*, 10(3). <https://doi.org/10.1371/journal.pone.0121729>
- [66] Jankovic, M. (2020). Contactless real-time heartbeat detection via 24 ghz continuous-wave doppler radar using artificial neural networks. *Sensors (Switzerland)* <https://doi.org/10.3390/s20082351>
- [67] Silver-Christiansen1999\_Book\_BiomaterialsScienceAndBiocompa. (n.d.).
- [68] Wang, S., Pohl, A., Jaeschke, T., Czaplik, M., Kony, M., Leonhardt, S., & Pohl, N. (2015). A novel ultra-wideband 80 GHz FMCW radar system for contactless monitoring of vital signs. *Proceedings of the Annual International Conference of the IEEE Engineering in Medicine and Biology Society, EMBS, 2015-November*, 4978–4981. <https://doi.org/10.1109/EMBC.2015.7319509>
- [69] Lakshmi, I. (2021). Anatomical photo representations for cardiac imaging training. In *Image Processing for Automated Diagnosis of Cardiac Diseases* (pp. 35–48). Elsevier. <https://doi.org/10.1016/B978-0-323-85064-3.00005-4>
- [70] Aardal, Ø., Paichard, Y., Brovoll, S., Berger, T., Lande, T. S., & Hamran, S. E. (2013). Physical working principles of medical radar. *IEEE Transactions on Biomedical Engineering*, 60(4), 1142–1149. <https://doi.org/10.1109/TBME.2012.2228263>
- [71] C. Gabriel, S. Gabriel, and E. Corthout, "The dielectric properties of biological tissues—I: Literature survey," *Phys. Med. Biol.*, vol. 41, pp. 2231–2249, Nov. 1996.
- [72] Martinek, R., Ladrova, M., Sidikova, M., Jaros, R., Behbehani, K., Kahankova, R., & Kawala-Sterniuk, A. (2021). Advanced bioelectrical signal processing methods: Past, present and future approach—Part I: Cardiac signals. In *Sensors (Vol. 21, Issue 15)*. MDPI AG. <https://doi.org/10.3390/s21155186>
- [73] Lee, H., Kim, B. H., Park, J. K., Kim, S. W., & Yook, J. G. (2020). A Resolution enhancement technique for remote monitoring of the vital signs of multiple subjects using a 24 GHz bandwidth-limited fmcw radar. *IEEE Access*, 8, 1240–1248. <https://doi.org/10.1109/ACCESS.2019.2961130>
- [74] N. S. NAMEROW, METHOD FOR MONITORING INTRASOMATIC CIRCULATORY FUNCTIONS AND ORGAN MOVEMENT, Dec. 16, 1969
- [75] Tworzyclo, P. (2016). Monitoring Breathing Using a Doppler Radar.
- [76] Shafiq, G., & Veluvolu, K. C. (2014). Surface chest motion decomposition for cardiovascular monitoring. *Scientific Reports*, 4. <https://doi.org/10.1038/srep05093>
- [77] Schallinger, L. E., Johnson, J., & Givot, B. (2010). Characterization of Tissue-Equivalent IVaterials for High-Frequency Applications (200 MHz to 20 GHz) Sung Kim.
- [78] I. Lakshmi, Chapter 3 - Anatomical photo representations for cardiac imaging training, Editor(s): Kalpana Chauhan, Rajeev Kumar Chauhan, *Image Processing for Automated Diagnosis of Cardiac Diseases*, Academic Press, 2021

- [79] Sapra A, Malik A, Bhandari P. Vital Sign Assessment. 2022 May 8. In: Stat Pearls [Internet]. Treasure Island (FL): Stat Pearls Publishing; 2022 Jan–. PMID: 31985994.
- [80] Yan, X., & Chowdhury, N. A. (2010). Electricity market clearing price forecasting in a deregulated electricity market. 2010 IEEE 11th International Conference on Probabilistic Methods Applied to Power Systems, PMAPS 2010, 36–41. <https://doi.org/10.1109/PMAPS.2010.5528949>
- [81] Tu, J., & Lin, J. (2016). Fast acquisition of heart rate in noncontact vital sign radar measurement using time-window-variation technique. *IEEE Transactions on Instrumentation and Measurement*, 65(1), 112–122. <https://doi.org/10.1109/TIM.2015.2479103>
- [82] <https://www.cvphysiology.com/uploads/images/HD002%20cardiac%20flow%20during%20systole-diastole.gif>
- [83] A. Ahmad, J. C. Roh, D. Wang and A. Dubey, "Vital signs monitoring of multiple people using a FMCW millimeter-wave sensor," 2018 IEEE Radar Conference (RadarConf18), 2018, pp. 1450-1455, doi: 10.1109/RADAR.2018.8378778.
- [84] Richardson M. The respiratory system. Part 4: breathing. *Nurs Times*. 2006 Jun 13-19;102(24):26-7. PMID: 16827043.
- [85] Ostadfar, A. (2016). Biofluid Dynamics in Human Organs. In *Biofluid Mechanics* (pp. 111–204). Elsevier. <https://doi.org/10.1016/b978-0-12-802408-9.00004-1>
- [86] Avram, R., Tison, G. H., Aschbacher, K., Kuhar, P., Vittinghoff, E., Butzner, M., Runge, R., Wu, N., Pletcher, M. J., Marcus, G. M., & Olgin, J. (2019). Real-world heart rate norms in the health eHeart study. *Npj Digital Medicine*, 2(1). <https://doi.org/10.1038/s41746-019-0134-9>
- [87] Lee YS, Pathirana PN, Steinfors CL, Caelli T. Monitoring and Analysis of Respiratory Patterns Using Microwave Doppler Radar. *IEEE J Transl Eng Health Med*. 2014 Oct 31;2:1800912. doi: 10.1109/JTEHM.2014.2365776. PMID: 27170871; PMCID: PMC4848092.
- [88] Light GA, Williams LE, Minow F, Sprock J, Rissling A, Sharp R, Swerdlow NR, Braff DL. Electroencephalography (EEG) and event-related potentials (ERPs) with human participants. *Curr Protoc Neurosci*. 2010 Jul;Chapter 6:Unit 6.25.1-24. doi: 10.1002/0471142301.ns0625s52. PMID: 20578033; PMCID: PMC2909037.
- [89] Park DS, Fishman GI. Development and Function of the Cardiac Conduction System in Health and Disease. *J Cardiovasc Dev Dis*. 2017;4(2):7. doi: 10.3390/jcdd4020007. Epub 2017 Jun 7. PMID: 29098150; PMCID: PMC5663314.
- [90] [https://www.netmeds.com/images/cms/wysiwyg/blog/2022/05/1651826489\\_electroencephalography\\_898x450.jpg](https://www.netmeds.com/images/cms/wysiwyg/blog/2022/05/1651826489_electroencephalography_898x450.jpg)
- [91] The global health observatory explores a world of health data. <http://www.who.int/data/gho>
- [92] Connor, G., & Melia, R. (2013). Electromagnetic Absorption by the Human Body from 1 to 15 GHz.
- [93] Aardal, Ø., Paichard, Y., Brovoll, S., Berger, T., Lande, T. S., & Hamran, S. E. (2013). Physical working principles of medical radar. *IEEE Transactions on Biomedical Engineering*, 60(4), 1142–1149. <https://doi.org/10.1109/TBME.2012.2228263>
- [94] Johnson, C. C., & Guy, A. W. (1972). Nonionizing electromagnetic wave effects in biological materials and systems. *Proceedings of the IEEE*, 60(6), 692–718. <https://doi.org/10.1109/PROC.1972.8728>

- [95] Parker, M. (2017). Radar Basics. *Digital Signal Processing* 101, 231–240. <https://doi.org/10.1016/B978-0-12-811453-7.00018-4>
- [96] Singh, Y. N., Singh, S. K., & Ray, A. K. (2012). Bioelectrical Signals as Emerging Biometrics: Issues and Challenges. *ISRN Signal Processing*, 2012, 1–13. <https://doi.org/10.5402/2012/712032>
- [97] Tworzydło, P. (2016). Monitoring Breathing Using a Doppler Radar.
- [98] UNIVERSITÉ DE MONTRÉAL. SYSTÈME MÉDICAL INTÉGRÉ DE RADAR POUR LA SURVEILLANCE DE PRÉCISION. MAÎTRISE ÈS SCIENCES APPLIQUÉES Lydia Chioukh, 2009.
- [99] Sacco, G., Piuze, E., Pittella, E., & Pisa, S. (2020). An FMCW radar for localization and vital signs measurement for different chest orientations. *Sensors (Switzerland)*, 20(12), 1–14. <https://doi.org/10.3390/s20123489>
- [100] Usta, M. B. (2021). Prediction of outcome in children with autism spectrum disorders. In *Neural Engineering Techniques for Autism Spectrum Disorder: Volume 1: Imaging and Signal Analysis* (pp. 1–8). Elsevier. <https://doi.org/10.1016/B978-0-12-822822-7.00001-6>
- [101] Palo F, Galati G, Pavan G, Wasserzier C, Savci K. Introduction to Noise Radar and Its Waveforms. *Sensors (Basel)*. 2020 Sep 11;20(18):5187. doi: 10.3390/s20185187. PMID: 32932959; PMCID: PMC7571191.
- [102] Levanon, N. (2003). Radar. *Encyclopedia of Physical Science and Technology*, 497–510. <https://doi.org/10.1016/B0-12-227410-5/00973-X>
- [103] Cheng, J. H., Yeh, J. F., Yang, H. Y., Tsai, J. H., Lin, J., & Huang, T. W. (2012). 40-GHz vital sign detection of heartbeat using synchronized motion technique for respiration signal suppression. *European Microwave Week 2012: "Space for Microwaves", EuMW 2012, Conference Proceedings - 42nd European Microwave Conference, EuMC 2012, 21–24*. <https://doi.org/10.23919/eumc.2012.6459289>
- [104] [https://commons.wikimedia.org/wiki/File:Cardiac\\_action\\_potential.png](https://commons.wikimedia.org/wiki/File:Cardiac_action_potential.png)
- [105] G. Brown ET AL. Apparatus for measuring electric field radiation from living bodies.
- [106] Tu, J., & Lin, J. (2016). Fast acquisition of heart rate in noncontact vital sign radar measurement using time-window-variation technique. *IEEE Transactions on Instrumentation and Measurement*, 65(1), 112–122. <https://doi.org/10.1109/TIM.2015.2479103>
- [107] Lv, W., He, W., Lin, X., & Miao, J. (2021). Non-contact monitoring of human vital signs using fmcw millimeter wave radar in the 120 ghz band. *Sensors*, 21(8). <https://doi.org/10.3390/s21082732>
- [108] Merline, A., & Thiruvengadam, S. J. (2013). Multiple-input multiple-output radar waveform design methodologies. In *Defence Science Journal* (Vol. 63, Issue 4, pp. 393–401). Defense Scientific Information and Documentation Centre. <https://doi.org/10.14429/dsj.63.2537>
- [109] Cardillo, E., & Caddemi, A. (2020). A review on biomedical mimo radars for vital sign detection and human localization. In *Electronics (Switzerland)* (Vol. 9, Issue 9, pp. 1–

15). MDPI AG. <https://doi.org/10.3390/electronics9091497>

## PUBLICATIONS

---

### Journals

[J1] Halima EL Grari, Tarek Djerafi. “On the limits of Doppler Radar in Vital Signs Detection,” will submit in IEEE as a journal article.

### Conferences

[C1] Halima EL Grari, Falk Tiago, Tarek Djerafi “Cardiac Arrhythmia Prediction Using Supervised Machine Learning Methods,” will submit in IEEE as a conference paper.